Cell Biology

Continuous endosomes form functional subdomains and orchestrate rapid membrane trafficking in trypanosomes

Reviewed Preprint

Revised by authors after peer review.

About eLife's process

Reviewed preprint version 2
February 22, 2024 (this version)

Reviewed preprint version 1
September 27, 2023

Sent for peer review
August 3, 2023

Posted to preprint server
July 20, 2023

Fabian Link, Alyssa Borges, Oliver Karo, Marvin Jungblut, Thomas Müller, Elisabeth Meyer-Natus, Timothy Krüger, Stefan Sachs, Nicola G. Jones, Mary Morphew, Markus Sauer, Christian Stigloher, J. Richard McIntosh, Markus Engstler

Department of Cell & Developmental Biology, Biocentre, University of Würzburg, 97074 Würzburg, Germany • Department of Biotechnology & Biophysics, Biocentre, University of Würzburg, 97074 Würzburg, Germany • Molecular, Cellular & Developmental Biology, University of Boulder, Colorado, USA • Imaging Core Facility, Biocentre, University of Würzburg, 97074 Würzburg, Germany

Abstract

Endocytosis is a common process observed in most eukaryotic cells, although its complexity varies among different organisms. In *Trypanosoma brucei*, the endocytic machinery is under special selective pressure because rapid membrane recycling is essential for immune evasion. This unicellular parasite effectively removes host antibodies from its cell surface through hydrodynamic drag and fast endocytic internalization. The entire process of membrane recycling occurs exclusively through the flagellar pocket, an extracellular organelle situated at the posterior pole of the spindle-shaped cell. The high-speed dynamics of membrane flux in trypanosomes do not seem compatible with the conventional concept of distinct compartments for early, late and recycling endosomes. To investigate the underlying structural basis for the remarkably fast membrane traffic in trypanosomes, we employed advanced techniques in light and electron microscopy to examine the three-dimensional architecture of the endosomal system. Our findings reveal that the endosomal system in trypanosomes exhibits a remarkably intricate structure. Instead of being compartmentalized, it constitutes a continuous membrane system, with specific functions of the endosome segregated into membrane subdomains enriched with classical markers for early, late, and recycling endosomes. These membrane subdomains can partly overlap or are interspersed with areas that are negative for endosomal markers. This continuous endosome allows fast membrane flux by facilitated diffusion that is not slowed by multiple fission and fusion events.

eLife assessment

This **important** study combines a range of advanced ultrastructural imaging approaches to define the unusual endosomal system of African trypanosomes. **Compelling** images reveal that, unlike a conventional set of compartments, the endosome in these protists forms a continuous membrane system with functionally distinct subdomains, as defined by canonical markers for early, late, and recycling endosomes. The findings compellingly support that the endocytic system in bloodstream stages has adapted to support remarkably high rates of membrane turnover necessary for immune complex removal and survival in the blood. This research is particularly relevant to those investigating infectious diseases

Introduction

Endocytosis research has traditionally focused on a limited number of organisms, primarily opisthokonts (including yeast and humans). Recently, using the extensive genetic and cell biological resources now available for studying numerous other organisms, studies on protists such as *Dictyostelium*, *Giardia*, *Toxoplasma* or trypanosomes have revealed remarkable deviations from the hitherto existing understanding of the processes of endo- and exocytosis described in textbooks (reviewed in Benchimol and de Souza, 2022; Link et al., 2021; McGovern et al., 2021; Vines and King, 2019). Looking at the distinct evolutionary solutions for endosomal recycling across different branches of the eukaryotes, these protists, and especially the parasites among them, are of particular interest.

Throughout their life cycle, parasites often encounter a series of inherently hostile environments. The arms race between the parasite and its host has resulted in coevolutionary processes characterized by intense reciprocal selective pressures. Although parasite and host use similar basic cell biological pathways, parasites have often optimised these, either to achieve maximum efficiency or to establish additional functions. In this regard, the endocytosis and membrane recycling mechanisms observed in African trypanosomes serve as a remarkable illustration of the exceptional functional adaptations exhibited by parasites in response to their specific host environments.

Trypanosoma brucei is a representative of the group Discoba, which diverged before the appearance of opisthokonts (Burki et al., 2020; Strassert et al., 2021). *T. brucei* is an exclusively extracellular parasite, that resists the harsh conditions within the bloodstream, interstitial fluids and lymph and thus thrives in the body fluids of its vertebrate host. Additionally, the cells have adapted to entirely distinct, yet equally challenging environments within the transmitting insect vector, *Glossina* (tsetse fly). Within the midgut of the fly, the trypanosomes proliferate to very high densities and, following a several week long journey, attach to the insect salivary glands before being injected back into the host skin during the bloodmeal of the tsetse (Rose et al., 2020).

The extracellular lifestyle of *T. brucei* renders the parasite vulnerable to constant attacks by the host's immune system. In response, these parasites have evolved a protective surface coat covering the entire plasma membrane (Cross, 1975). This coat comprises a single type of variant surface glycoprotein (VSG) and forms the basis of antigenic variation (Mugnier et al., 2016). *T. brucei* possesses hundreds of VSG genes that encode structurally similar yet antigenically distinct proteins (Taylor and Rudenko, 2006). However, only one VSG gene is expressed at a time,

originating from a polycistronic expression site located at the telomere of the chromosomes (Becker et al., 2004; Chaves et al., 1999). The stochastic switching to the expression of a new VSG guarantees that the parasites remain ahead of the host immune response.

Antigenic variation is not the sole defense strategy employed against the host's immune reaction. During immune attack, parasites actively remove anti-VSG antibodies from their cell surface. This process of antibody clearance is driven by hydrodynamic drag forces resulting from the continuous directional movement of trypanosomes (Engstler et al., 2007). The VSG-antibody complexes on the cell surface are dragged against the swimming direction of the parasite and accumulate at the posterior pole of the cell. This region harbours an invagination in the plasma membrane known as the flagellar pocket (FP) (Gull, 2003; Overath et al., 1997). The FP, which marks the origin of the single attached flagellum, is the exclusive site for endo- and exocytosis in trypanosomes (Gull, 2003; Overath et al., 1997). Consequently, the accumulation of VSG-antibody complexes occurs precisely in the area of bulk membrane uptake. For the process of antibody clearance to function efficiently, several conditions must be met. The VSG coat must be densely packed to prevent immune recognition of non-variant surface proteins, VSG must be highly mobile to allow the drag forces to take effect, and endocytosis must be sufficiently rapid to internalize the VSG-antibody complexes effectively. Furthermore, endosomal sorting and membrane recycling must keep pace with the bulk membrane uptake to maintain membrane balance. In fact, the VSG coat is as densely packed as physically possible (Hartel et al., 2016) and VSG molecules possess a flexible C-terminal domain attached via a GPI-anchor to the outer leaflet of the plasma membrane (reviewed in Borges et al., 2021). This lipid anchoring enables the highly dynamic behaviour of the VSG coat (Bartossek et al., 2017), further facilitated by N-glycans that insulate VSG molecules, thereby minimizing protein-protein interactions (Hartel et al., 2016). VSG molecules exhibit diffusion on the plasma membrane with coefficients that enable fast randomization (Hartel et al., 2016; Schwebs et al., 2022). This rapid VSG diffusion is precisely balanced with membrane recycling kinetics, with one surface equivalent being internalized and recycled within 12 minutes (Engstler et al., 2004). This exceptionally fast endocytosis is crucial for antibody clearance.

To summarize, *T. brucei* has evolved a series of interconnected cell biological adaptations in order to evade the immune system, ranging from a highly polarized cell structure and constant directional motion to the generation of a variable, densely packed yet highly mobile cell surface coat, as well as an unusually rapid endocytosis machinery. The strong selective pressure acting on trypanosomes has led to the integration and coordination of seemingly unrelated features, such as cell motility, surface protein dynamics, clathrin-mediated endocytosis, protein sorting, and membrane recycling. This illustrates the extraordinary cell biology of parasitic protozoa, which offers functional linkages beyond that of yeast or mammalian cells.

In *T. brucei*, the process of endocytosis (reviewed in Link et al., 2021) begins with the formation of clathrin-coated vesicles (CCVs) at the flagellar pocket membrane (Allen et al., 2003; Morgan et al., 2001). Subsequently, both membrane-bound VSG and fluid-phase cargo pass through early endosomes (EE) (Engstler et al., 2004; Grünfelder et al., 2003). From this compartment, both either move directly to the recycling endosomes (RE) and return to the cell surface or first pass from the EE to the late endosomes (LE) before returning to the surface via the RE (Engstler et al., 2004). Alternatively, fluid-phase cargo can be directed from LEs to the lysosome for degradation (Engstler et al., 2004). In comparison, less is known about the biosynthetic pathway to the lysosome. Endogenous proteins like TbCatL, a soluble thiol protease, and p67, a membrane glycoprotein, are segregated from secretory cargo in the Golgi apparatus. They are then transported out of the Golgi, probably in a clathrin-dependent manner (Tazeh et al., 2009). An alternative route to the lysosome was discovered by disrupting transport signals in endogenous proteins, for example by blocking of GPI anchor addition to VSGs (Triggs and Bangs, 2003).

Similar to other eukaryotic organisms, the trafficking process through various endosomal compartments is regulated by a core set of three small Rab-GTPases (Ackers et al., 2005). TbRab5 and TbRab11 are responsible for controlling trafficking through the early and recycling endosomes, respectively (Field et al., 1998; Hall et al., 2005; Pal et al., 2003). TbRab7 plays a role in regulating late endocytic trafficking to the lysosome, but does not appear to be involved in the biosynthetic trafficking of either native lysosomal proteins or default reporters (Silverman et al., 2011). TbRab5A-positive endosomal structures have been described by immuno-electron microscopy as circular or elongated cisternae, while TbRab7-positive structures exhibit an irregular shape (Engstler et al., 2004; Grünfelder et al., 2003; Overath and Engstler, 2004). Additionally, TbRab11-positive structures are characterized as either elongated cisternae or disk-shaped exocytic carriers (Grünfelder et al., 2003). Apart from exocytic carriers, the exocyst is currently the only proposed mediator of exocytosis (Boehm et al., 2017).

A thorough examination of the kinetics of endosomal recycling has validated the rapid passage through various endosomal compartments (Engstler et al., 2004; Grünfelder et al., 2003). However, these analyses have not addressed how the kinetics can be reconciled with the occurrence of multiple fission and fusion events that are thought to accompany endosomal transport through these compartments.

Here, we have employed a comprehensive set of techniques to scrutinize the ultrastructure of specific endosomal subdomains in *T. brucei*. In addition to utilizing electron tomography, super-resolution fluorescence microscopy and colocalization analysis, we have introduced Tokuyasu sectioning for 3D immuno-electron microscopy. These tools allowed us to elucidate the structural basis for the remarkable speed of endosomal recycling in trypanosomes.

Results

The endosomal apparatus of *T. brucei* is a large intricate structure

In order to generate an overview of the endosomal ultrastructure in bloodstream form (BSF) trypanosomes, we performed electron tomography after fluid phase cargo uptake assays with horseradish peroxidase (HRP) and ferritin (**Figure 1**, Supplementary movie 1). Fluid phase cargo was selected as it ensures a comprehensive labelling of all endosomal compartments (Engstler et al., 2004). Following HRP/ferritin endocytosis, the cells were fixed and embedded in Epon resin. To visualize HRP, photooxidation with 3,3'-diaminobenzidine (DAB) was employed before acquiring tomographic data (**Figure 1 A, B**, and **D**). Analysis of the reconstructed electron tomograms of various BSF cells revealed a morphologically intricate system of endosomes comprised of interconnected and fenestrated membrane networks. The main endosome, spanning the posterior region of the cell from the vicinity of the flagellar pocket (FP) to the Golgi apparatus, exhibited elongated (**Figure 1 A** and **B**) and circular membrane sheets (**Figure 1 C** and **D**), encompassing a volume with a diameter of approximately 2 µm and a length of 4 µm. The localization of endosomes was strictly confined to the posterior cytoplasm. Their precise positioning, however, appeared to be flexible, indicating a lack of direct and rigid connection with the microtubule cytoskeleton. This observation is not surprising, as there are no reports of cytoplasmic microtubules in trypanosomes. All microtubules appear to be either subpellicular or within the flagellum. However, it is very likely that a scaffold is necessary to maintain the intricate membrane structure of the endosomal system, especially given the constant deformation of the cell body by the beating of the attached flagellum. The electron tomograms further suggest that the large size of the endosomes may render them unable to pass through the space between the nucleus and pellicular microtubules. Another notable finding was the proximity of endosomes to the Golgi apparatus (**Figure 1 A** and **B**), suggesting a potential involvement of the endosomal system in post-Golgi transport.

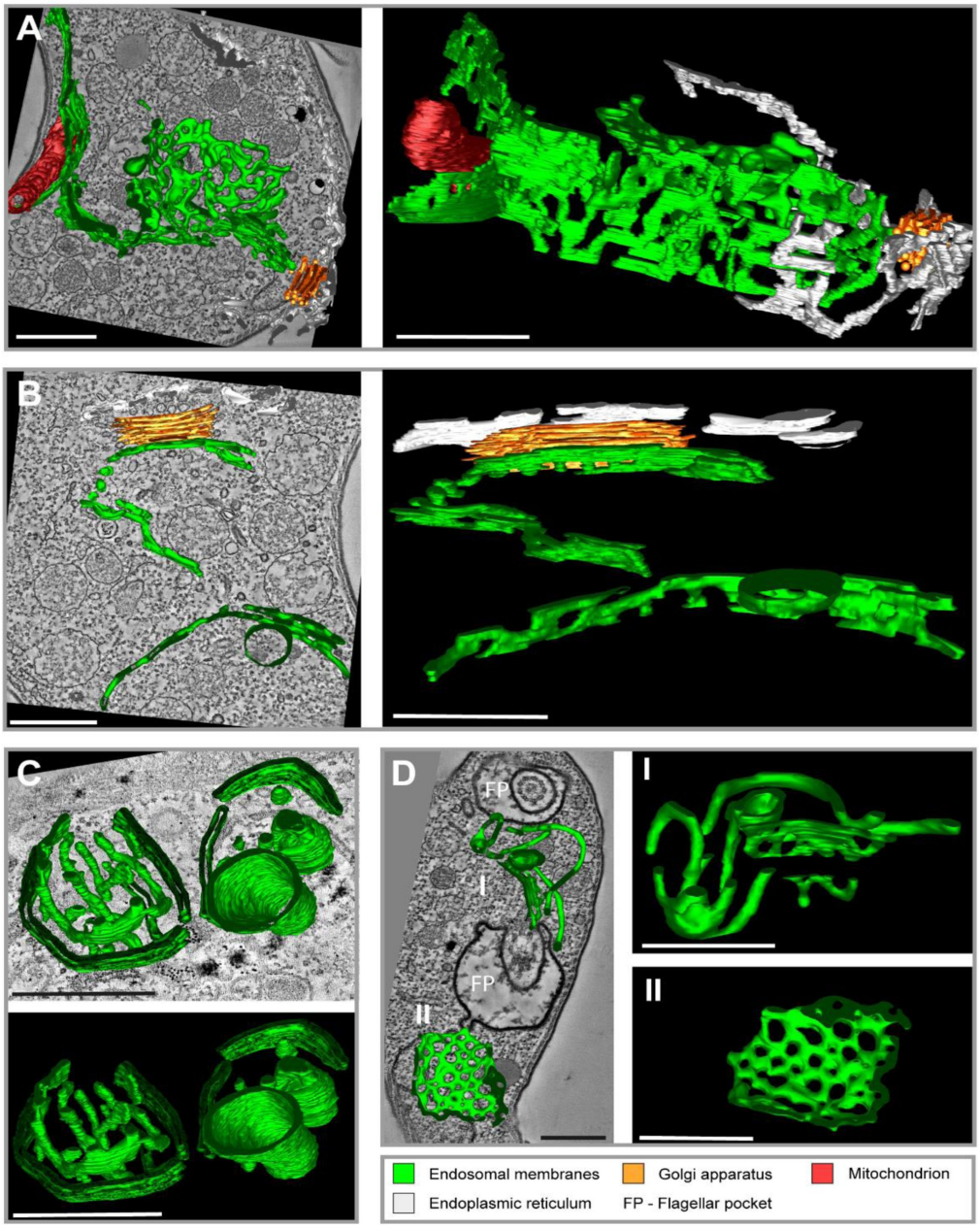

Figure 1.

Tomographic reconstructions of the endosomal apparatus of *T. brucei* after cargo uptake reveals a large and mostly continuous membrane system.

(A) Elongated and highly fenestrated endosomal sheets and palisades. **(B)** Elongated and slightly fenestrated endosomes. **(C)** Large circular endosomal cisternae. **(D)** Two different substructures are displayed: one contains tubular palisades (I) while the other one is a heavily fenestrated sheet (II). HRP endocytosis and DAB photooxidation were performed prior to tomogram acquisition (A, B and D). Ferritin endocytosis was performed prior to tomogram acquisition (C). All sections are 250 nm thick. The reconstructions (A) and (D) are based on three and two sections, respectively. The reconstructions (C) and (D) are based on one section each. The section and corresponding tomogram (C) originate from the same sample block as the image in **Figure 4** I from Engstler et al. (2004). Endosomal membranes are shown in green. The endoplasmic reticulum is visualised in white colour. The Golgi apparatus is labelled in orange and the mitochondrion is shown in red. Abbreviation: flagellar pocket (FP). Scale bars: 500 nm. Movies corresponding to panel A-D can be found here: A) z-stack, 3D model; B) z-stack, 3D model; C) z-stack, 3D model; D) z-stack, 3D model. The tomograms provided serve as a representative sample among the 37 tomograms that were recorded.

To investigate potential negative impacts of processing steps (cargo uptake, centrifugation, washing) on endosomal organization, we directly fixed cells in the cell culture flask, embedded them in Epon, and conducted electron tomography. The resulting tomograms revealed endosomal organization consistent with that observed in cells fixed after processing (see Supplementary movie 2, 3, and 4).

In summary, electron tomography analyses provided evidence that the endosomal system in BSF cells is a complex, flexible, and largely continuous membrane network.

Super-resolution microscopy reveals the endosomal apparatus as a largely continuous structure

To be able to do specific labelling of the endosomal compartment, we first tested the potential of various super-resolution light microscopy techniques to resolve and corroborate the structure of the entire endosomal compartment (**Figure 2** and S1). To allow the identification of endosomes, we utilized the marker protein EP1 that had previously been demonstrated to label the entire endosome and flagellar pocket of bloodstream form trypanosomes (Engstler and Boshart, 2004). EP1, a cell surface protein found in insect stage trypanosomes, is mostly excluded from the VSG coat of bloodstream form (BSF) trypanosomes.

To utilize EP1 as an endosomal membrane marker in *direct* stochastic optical reconstruction microscopy (*d*STORM) (Heilemann et al., 2008), an EP1::HaloTag expressing cell line was generated (Figure S2). The transgenic parasites were then labelled with a HaloTag ligand conjugated to Alexa Fluor™ 647 (custom conjugated, see Methods), and imaged in 100 mM MEA photo-switching buffer (Figure S1).

As expected, the EP1::HaloTag signal was localized in the posterior region of the cell, between the nucleus and kinetoplast (Figure S1, I – II). Although the entire endosomal compartment seemed to be labelled and gave the appearance of a largely connected system (Figure S1, III – IV), the labelling density was not consistently strong, resulting in occasionally thin membrane bridges (Figure S1, upper row, image IV, indicated by an arrow). In addition, the 3D volume of the labelled region was too large (approx. 4 x 4 x 5 µm) to be completely captured by single-molecule localization microscopy. On top of that, not all cells exhibited an EP1::Halo signal, indicating heterogeneous gene expression within the population (Figure S1, lower row, lower cell).

To overcome the non-uniform labelling density based on an endogenous marker protein and to be able to capture the entire 3D volume of the parasite, a combination of dextran uptake assays and expansion microscopy (Chen et al., 2015) was performed to visualize the endosomes. The fluorescently labelled dextran was observed in the posterior region between the nucleus and kinetoplast in all cells (**Figure 2 A**). The expanded and unexpanded cells revealed elongated cable-like structures representing the endosomes, spanning from the flagellar pocket to the vicinity of the nucleus. The expansion process improved the resolution of the structure, allowing for the visualization of potential circular cisternae (**Figure 2 A**, middle row, image III, arrow). While the flagellar pocket labelling was visible in nearly all unexpanded cells, not all expanded cells exhibited a corresponding signal (**Figure 2 A**). To improve the resolution even further, we performed structured illumination microscopy (SIM) on expanded cells (**Figure 2 B**). The result also demonstrated a largely continuous dextran signal between the nucleus and the kinetoplast, indicating the continuity of the endosomal structures.

To determine the expansion factor, the diameter of the flagellar pocket and the length of the endosomes were measured in multiple expanded and unexpanded cells (**Figure 2 C**). The median diameter of the fluorescence signal corresponding to the flagellar pocket increased from 0.84 µm to 3.08 µm, resulting in an expansion factor of 3.6. The median length of the endosomes increased from 2.51 µm to 7.88 µm, yielding an expansion factor of 3.1.

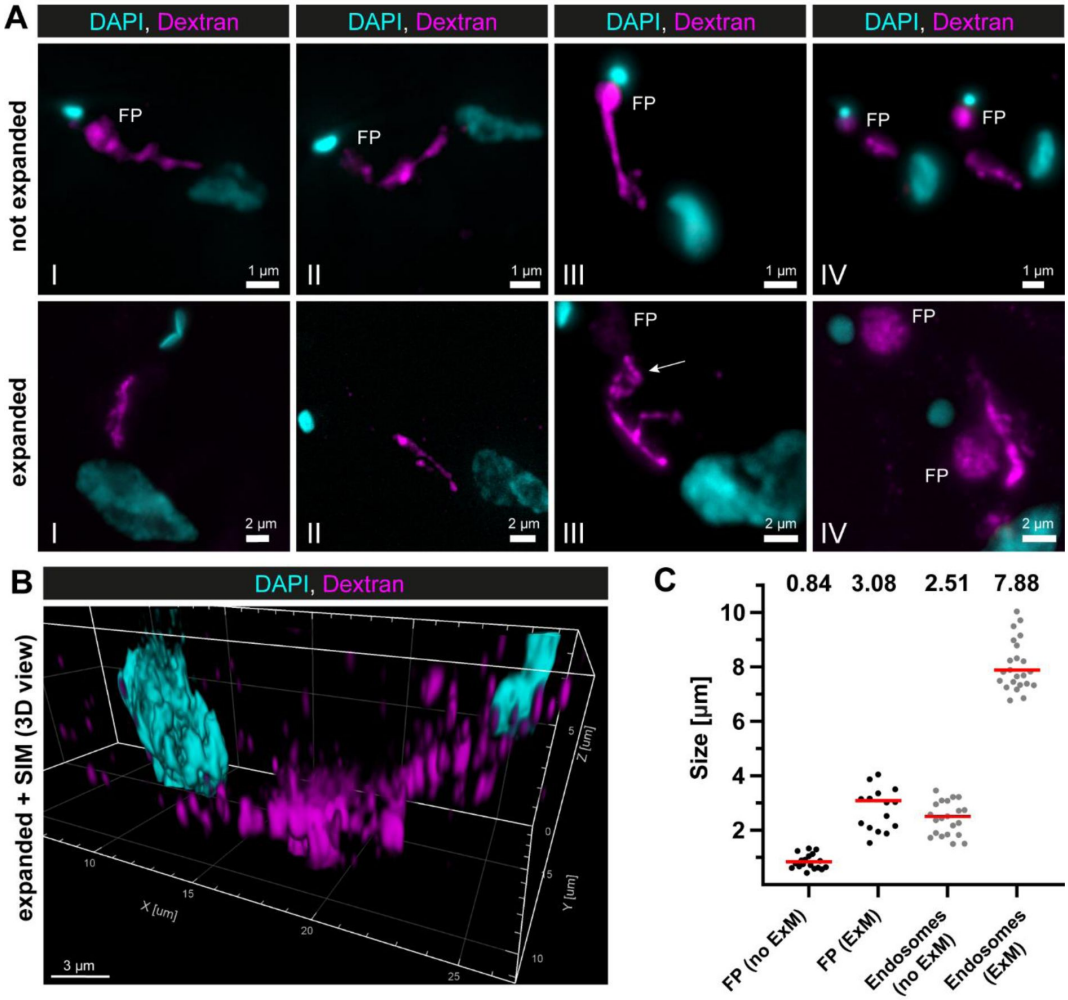

Figure 2.

Super-resolution light microscopy reveals continuous endosomal membranes.

(A) Visualisation of the endosomal system in *T. brucei* using expansion microscopy. Bloodstream form cells were pulsed with dextran conjugated to Alexa488 and fixed with 4 % formaldehyde and 0.2 % glutaraldehyde. Shown are exemplary images (I – IV) of not expanded and expanded cells imaged using widefield microscopy. All images represent a merge of DAPI staining (cyan) and dextran signal (magenta). Flagellar pockets (FP) are annotated. **(B)** 3D presentation of the endosomal system using a combination of expansion microscopy and structured illumination microscopy (SIM). The same gels as imaged in (B) were analysed with SIM. The 3D presentation was generated using the IMARIS package (Bitplane). **(C)** Scatter plot of the quantification of the expansion factor. The diameter of the fluorescence signal corresponding to flagellar pocket (FP) and length of the endosomes were measured in multiple not expanded (no ExM) and expanded cells (ExM) (n ≥ 15). The median values are indicated as red bars and the corresponding numbers are shown in the upper part of the panel.

In summary, super-resolution microscopy using a transgenic marker cell line and cargo uptake assays supported the possibility that in trypanosomes endosomes are largely continuous.

Quantitative 3D colocalization analysis reveals overlaps between early, late and recycling endosomal marker proteins

To functionally characterize different components of the endosomal system, specific antibodies against the endosomal marker proteins TbRab5A (early endosomes), TbRab7 (late endosomes), and TbRab11 (recycling endosomes) were generated and validated (Figure S3). Immunofluorescence assays were conducted, and the samples were imaged using 3D widefield microscopy. For quantitative colocalization analyses the previously established endosomal marker EP1::GFP (Engstler and Boshart, 2004) was used to define the entire endosomal compartment as the region of interest (ROI) (**Figure 3**).

The EP1::GFP fluorescence revealed a variable number of high intensity signals, surrounded, and connected by weaker signals (**Figure 3 A, I**). The fluorescence of the TbRab marker proteins was present in foci of varying numbers, sizes, and intensities (**Figure 3 A, II – IV**). The fluorescence signals for all three marker proteins were within the ROI defined by EP1. The visualization as maximum intensity projections (MIP) suggested that the different subdomains exhibited a low degree of colocalization and could represent physically distinct compartments for early, late, and recycling endosomes (**Figure 3 A, V**). To quantitate this finding, 3D objects were generated from the fluorescent signals for colocalization analysis using IMARIS (**Figure 3 A, VI – X**). These objects showed areas of unique staining as well as partially overlapping regions. The pairwise colocalization of different endosomal markers is shown in **Figure 3 A**, XI - XIII and **3 B**. The different cells in **Figure 3 B** were chosen to represent the dynamic nature of the labelled structures. Consequently, the selected cells provide diverse examples of how the labelling can appear.

For the colocalization analysis, the EP1::GFP objects were masked and used as a 3D ROI in IMARIS. The colocalization matrix (**Figure 3 C**) showed that TbRab5A and TbRab7 exhibited the highest signal overlap, with approximately 53 % volume in both combinations. While 35 % of the volume of TbRab5A was colocalized with TbRab11, 26.5 % of the volume of TbRab11 was colocalized with TbRab5A. The differences in colocalization volumes can be attributed to the larger volume of the TbRab11 positive compartment. Similar observations were made for the combination of TbRab7 and TbRab11. While 45 % of the volume of TbRab7 was colocalized with TbRab11, 29.9 % of the volume of TbRab11 was colocalized with TbRab7. Furthermore, the different marker combinations yielded comparable moderate correlation coefficients (Pearson) ranging from 0.37 (TbRab5A and TbRab11) to 0.43 (TbRab5A and TbRab7) (**Figure 3 D**).

In summary, the quantitative colocalization analyses revealed that on the one hand, the endosomal system features a high degree of connectivity, with considerable overlap of endosomal marker regions, and on the other hand, TbRab5A, TbRab7, and TbRab11 also demarcate separated regions in that system. These results can be interpreted as evidence of a continuous endosomal membrane system harbouring functional subdomains, with a limited amount of potentially separated early, late or recycling endosomes.

The endosomal markers TbRab5A, TbRab7 and TbRab11 are present on the same membranes

To investigate the potential functional sub-compartmentalization of endosomes in trypanosomes, we conducted immunogold assays on Tokuyasu cryosections. We defined gold particles that were 30 nm or closer to a membrane as membrane-bound, considering a conservative calculation where two IgG molecules, each 15 nm in size, are positioned between the bound epitope and the gold particle (**Figure 4**, panel A). Consequently, gold particles located further away may

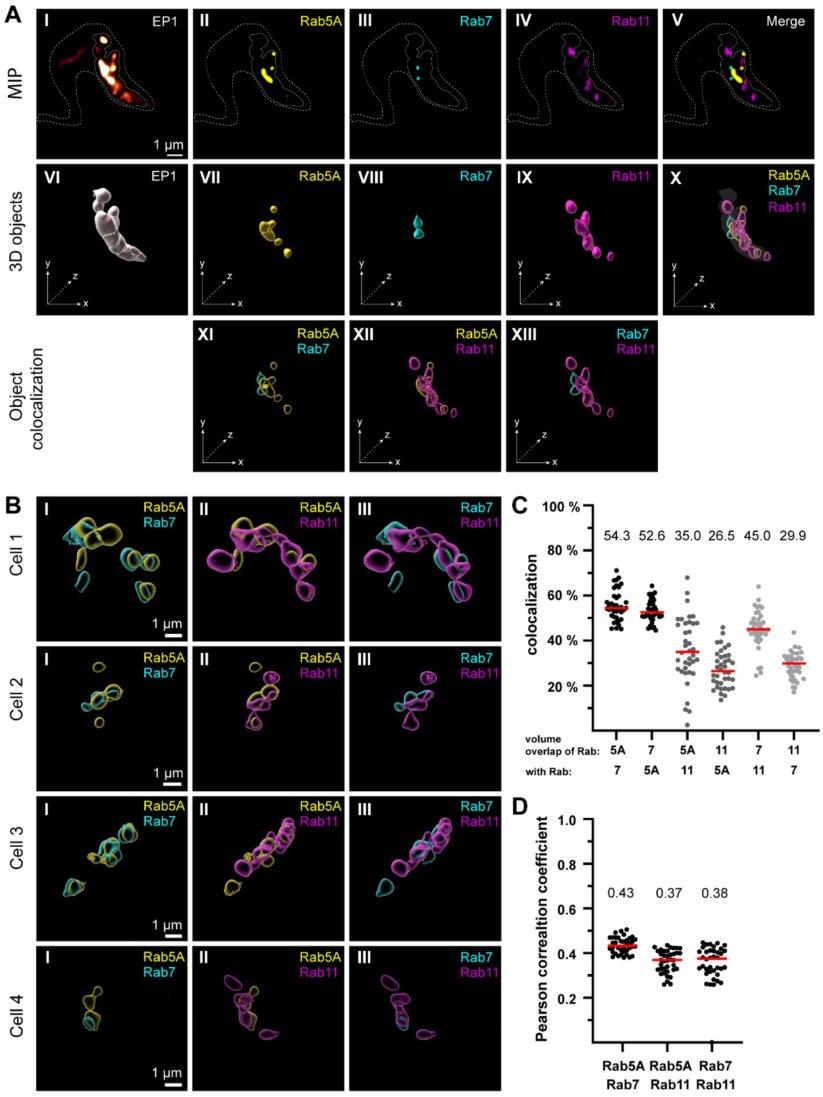

Figure 3.

The endosomal markers TbRab5A, TbRab7, and TbRab11 partly colocalize in the posterior region of the cell.

(A) The experimental workflow, from fluorescence images to object generation and quantitative 3D colocalization analysis, is exemplified. EP1::GFP (I) expressing cells were fixed and labelled with anti-TbRab5A (II), anti-TbRab7 (III) and anti-TbRab11 (IV) antibodies and imaged using widefield microscopy. Upper row: maximum intensity projections (MIP) for each individual fluorescence channel (I – IV) as well as a merge of all three anti-TbRab marker channels (V). The outline of the cell is shown by a dashed line (I - V) and the region of interest (endosomal system) is presented by a solid line (I - V). Middle row: Corresponding 3D objects to display the region of interest (VI) and the TbRab marker objects (VII – IX). The merge of all objects confirmed that the TbRab marker objects are located within the region of interest (X). Lower row: Colocalization of the objects representing TbRab5A and TbRab7 (XI), TbRab5A and TbRab11 (XII), TbRab7 and TbRab11 (XIII). The x-, y- and z-axes are indicated to support the three-dimensional view. **(B)** Object colocalization shown for additional cells. The colocalization of TbRab5A and TbRab7 (I), TbRab5A and TbRab11 (II), and TbRab7 and TbRab11 (III) is shown for different cells. (Cells 1 – 4). **(C - D)** Quantification of colocalization analysis for TbRab marker combinations. The colocalization function of IMARIS was used for the quantification. The EP1 surfaces defined the ROI (see panel A) and the automatic thresholding function (Costes et al., 2004) ensured minimal user bias. Each data point (n = 38) represents a field of view with 30 – 40 cells, corresponding to a total number of ~ 1,200 analysed cells. The median is highlighted with a red line and the corresponding number is written on top of the dataset. **(C)** Scatter plot of the colocalization analysis for the different TbRab marker combinations using the percentage of volume overlap. **(D)** Scatter plot of the colocalization analysis for the different TbRab marker combinations using the Pearson correlation coefficient.

represent cytoplasmic TbRab proteins or, as the "linkage error" can also occur in the z-plane, correspond to membranes that are not visible within the 55 nm thickness of the cryosection (**Figure 4**, panel C, arrows). The immuno-labelled structures exhibited a range of architectural features, including vesicular and tubular cisternae with circular or elongated shapes (**Figure 4**, **5**, **6**). The tubular structures had a thickness of 20 – 30 nm and extended up to a few microns in length (with the longest example shown in **Figure 5**, panel F, arrow). Vesicular shapes were observed in various sizes ranging from 30 nm to 135 nm in diameter.

While there were endosomal structures exclusively labelled with TbRab5A or TbRab7 (**Figure 4 D, E**, and **G**), a significant number of endosomal structures were labelled with both marker proteins (**Figure 4, B - G**). In contrast to TbRab5A and TbRab7, TbRab11 tended to form signal clusters on elongated structures (**Figure 5 A, B**, and **D**; **Figure 6 D - F**). TbRab11 was observed together with TbRab5A (**Figure 5 A - F**) or TbRab7 (**Figure 6 A - G**) on the same endosomal membranes, but it was also found as the sole marker on other endosomal membranes (**Figure 5 B, D, F**; **Figure 6 C** and **G**). The structures with a disk shape and positive for TbRab11 (**Figure 5 F**) were identified as exocytic carriers, as previously described in Grünfelder et al. (2003). Another noteworthy observation was that long elongated structures tended to have no or only weak labelling with any of the TbRab markers (**Figure 5**, panel F, arrow). To exclude potential artifacts, both gold size combinations were utilized for all marker combinations.

In summary, the exemplary images shown in **Figures 4**, **5** and **6** demonstrate the colocalization of TbRab5A, TbRab7 and TbRab11 on the same membranes, suggesting that the endosomal membrane system is unlikely to consist of distinct and independent compartments for early, late and recycling endosomes.

To confirm that the analysed membrane structures indeed represent endosomal membranes, we conducted cargo uptake assays and anti-VSG immunogold labelling (**Figure 7**). Trypanosomes were either pulsed with fluid-phase cargo (BSA; **Figure 7, A - C**) or cargo was taken up by receptor-mediated endocytosis (transferrin, Tf; **Figure 7, D - F**), and the sections were subsequently labelled with anti-TbRab antibodies. BSA and transferrin perfused the entire endosomal system, with the conjugated 5 nm gold particles visible inside the endosomal structures (**Figure 7, A - F**). Moreover, gold particles were observed within vesicles (**Figure 7, B** and **D**) and accumulated within the lysosome (**Figure 7, A** and **B**). In another set of experiments, the parasites were not pulsed with cargo markers, but the sections were labelled with anti-VSG and anti-TbRab antibodies (**Figure 7, G - I**). The anti-VSG antibodies decorated the entire plasma membrane (**Figure 7, G**) as well as intracellular membrane structures (**Figure 7, G - I**). The different TbRab marker proteins were found on the same membrane structures as the cargo markers or the anti-VSG antibodies (**Figure 7**, all panels). In summary, the use of cargo markers and antibodies targeting VSG and endosomal marker proteins confirmed the identity of the trypanosome endosomes.

3D Tokuyasu demonstrates that trypanosomes have continuous endosomal membranes

Following the visualization of continuous endosomal membranes through cargo uptake assays in Epon resin sections (**Figure 1**), we aimed to confirm these findings using 3D immuno-electron microscopy on cryosections (**Figure 8**). Cryosections with a thickness of 250 nm were labelled with antibodies against TbRab5A, TbRab7, and TbRab11. The 3D reconstructions provided an in-depth view of the interconnected circular and tube-like structures. Although the tomograms represented only a 250 nm thick section of a cell, it was evident that the membrane system likely exhibited further connections above and below the field of view. This assumption was confirmed by our experiments with conventional electron tomography. The 3D Tokuyasu method effectively highlighted the interconnectedness of these structures, expanding upon the observations from 2D

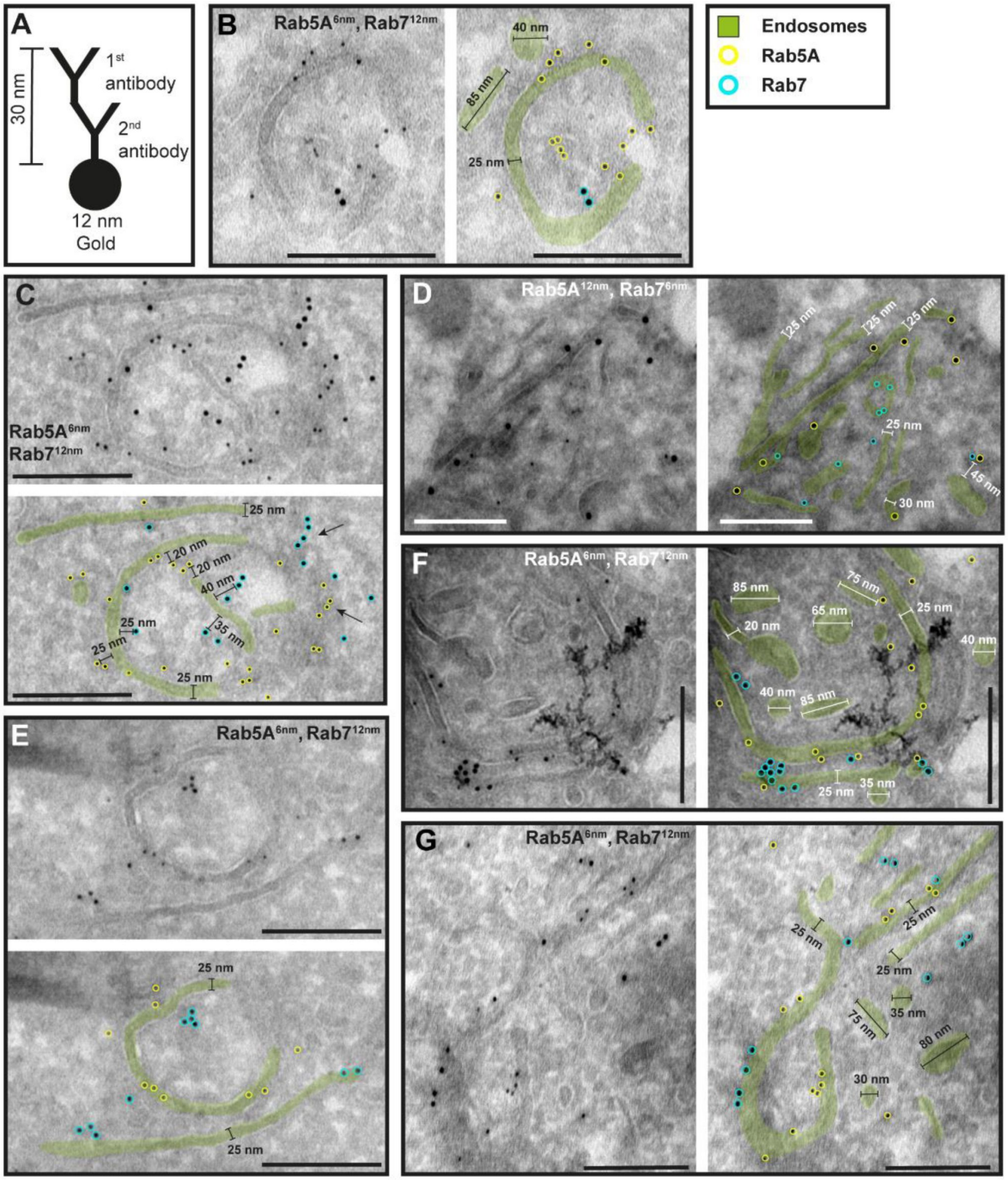

Figure 4.

The endosomal markers TbRab5A and TbRab7 are present on the same membrane.

(A) Schematic representation of antibody binding to visualise the maximum linkage error of 30 nm between a bound epitope and the gold particle. **(B - G)** Electron micrographs of cryosections labelled with rat anti-TbRab5A and guinea pig anti-TbRab7 antibodies and visualized with 6 or 12 nm gold-coupled secondary antibodies. For each panel an annotated and an unedited version of the image is presented. Endosomes are highlighted in green. Gold particles corresponding to TbRab5A signals are labelled in yellow. Gold particles corresponding to TbRab7 signals are highlighted in cyan. Scale bars: 200 nm. The images shown are representative examples drawn from over 300 micrographs generated in four distinct labelling experiments.

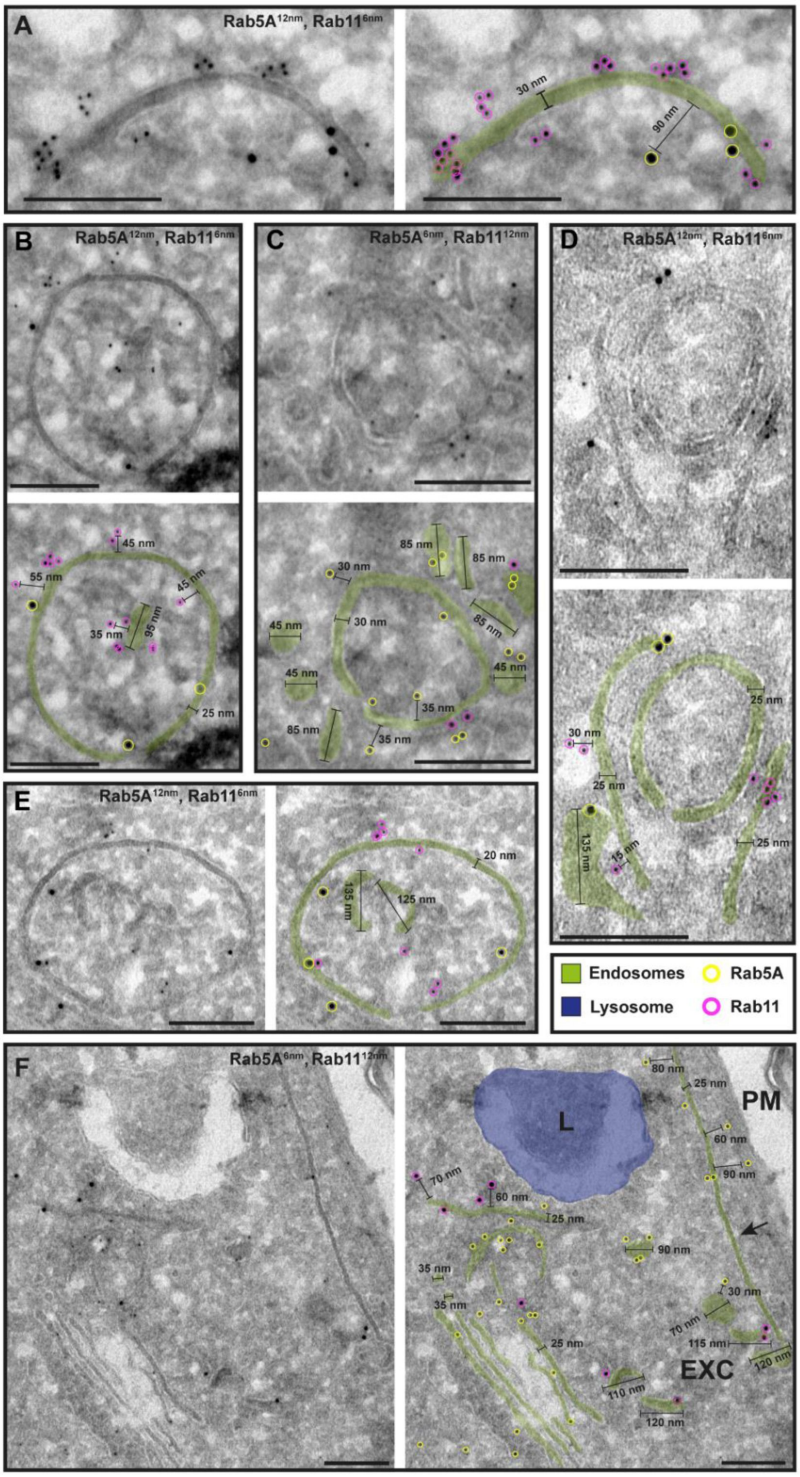

Figure 5.

The endosomal markers TbRab5A and TbRab11 are present on the same membranes.

(A - F) Electron micrographs of cryosections labelled with rat anti-TbRab5A and rabbit anti-TbRab11 antibodies and visualized with 6 or 12 nm gold-coupled secondary antibodies. For each panel an annotated and an unedited version of the image is presented. Endosomes are marked in green, and the lysosome is highlighted in blue. Gold particles are marked in yellow (TbRab5A) and in magenta (TbRab11). Scale bars: 200 nm. Exocytic carrier (EXC), lysosome (L), plasma membrane (PM). The displayed images are representative examples drawn from over 300 images generated in four distinct labelling experiments.

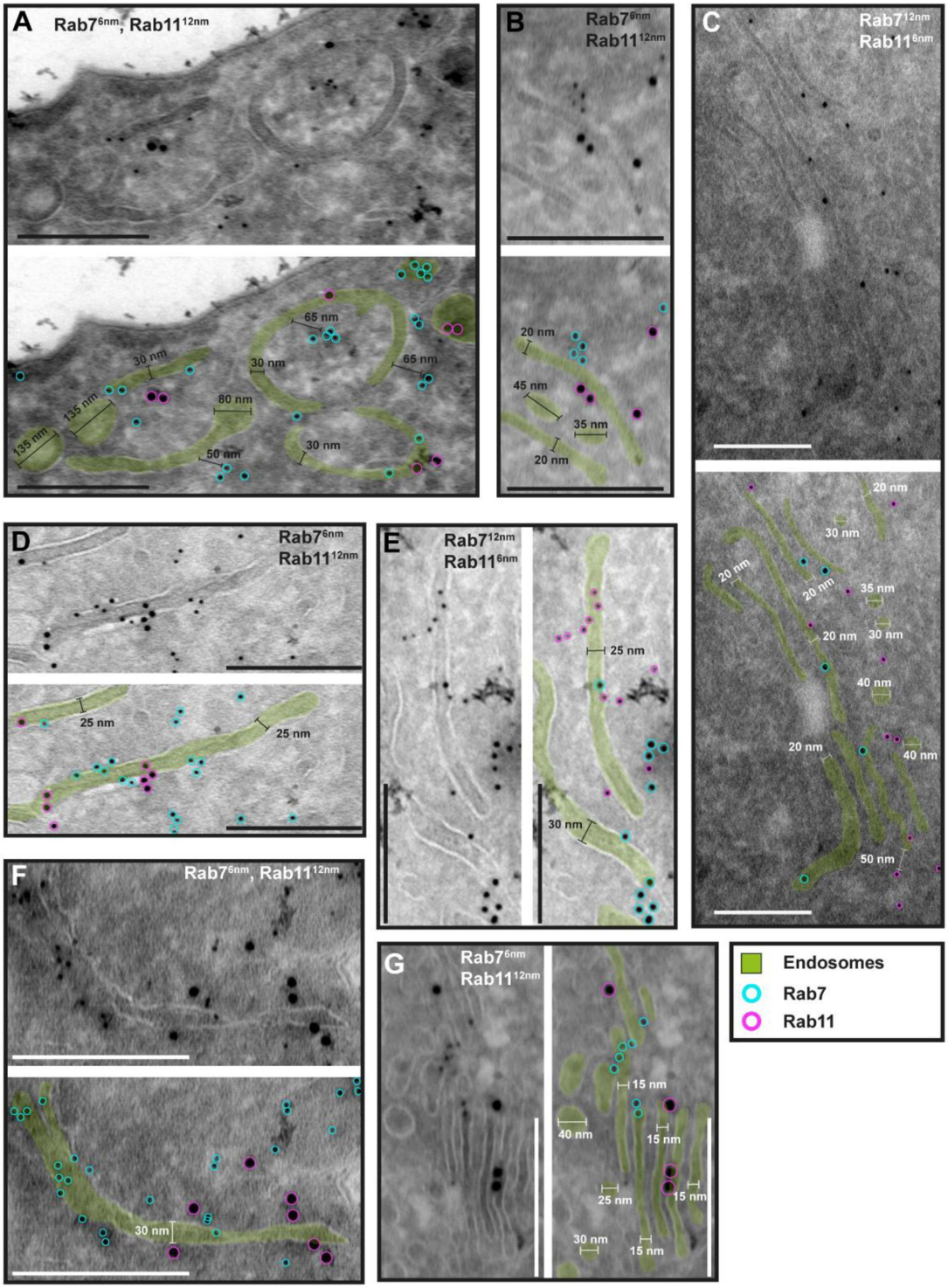

Figure 6.

The endosomal markers TbRab7 and TbRab11 are present on the same membranes.

(A - G) Electron micrographs of cryosections labelled with guinea pig anti-TbRab7 and rabbit anti-TbRab11 antibodies visualized with 6 or 12 nm gold-coupled secondary antibodies. For each panel an annotated and an unedited version of the image is presented. Endosomes are highlighted in green. Gold particles are labelled in cyan (TbRab7) and in magenta (TbRab11). Scale bars: 200 nm. The displayed images are representative examples drawn from over 200 images generated in three distinct labelling experiments.

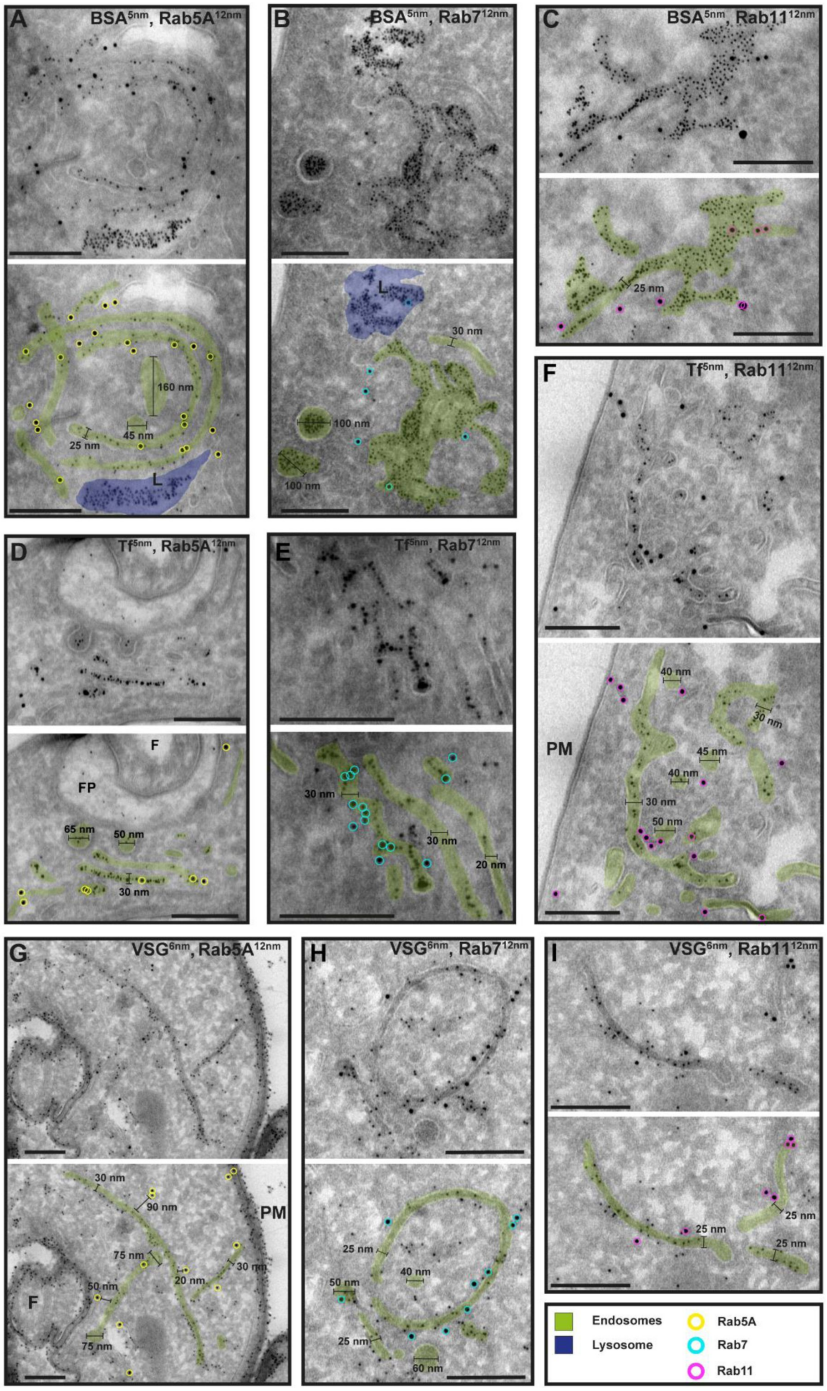

Figure 7.

Cargo uptake and anti-VSG immunogold labelling confirm the endosomal identity.

(A – I) Electron micrographs of cryosections labelled with anti-TbRab5A (yellow), anti-TbRab7 (cyan) or anti-TbRab11 (magenta) antibodies and 12 nm gold-conjugated secondary antibodies. For each panel an annotated and an unedited version of the image is presented. Endosomes are highlighted in green, the lysosome in blue. Parasites were incubated with 5 nm gold-conjugated BSA **(A – C)** or transferrin (Tf) **(D – F),** prior to fixation, sectioning and immunolabelling. BSA and transferrin cargo was observed in vesicles, endosomes, and lysosome. **(H – I)** Cells were labelled with anti-VSG antibodies and 6 nm gold-conjugated secondary antibodies. (F), flagellum, (FP) flagellar pocket, (PM) plasma membrane, (L) lysosome. Scale bars: 200 nm. The displayed images are representative examples drawn from over 50 images generated in three distinct labelling experiments.

analyses. Interestingly, these tomograms did not exhibit the fenestration pattern identified in traditional electron tomography. We suspect that this is due to methodological reasons. The Tokuyasu procedure uses only aldehydes to fix all structures. Consequently, effective fixation of lipids occurs only through their association with membrane proteins. Thus, the lack of visible fenestration is likely due to possible loss of lipids during incomplete fixation.

We observed endosomes decorated with different TbRab signals, supporting our assumption that functional subdomains exist within the same endosomal membrane system (**Figure 8, A** II and III, B II). It is worth noting that smaller gold particles demonstrated better penetration of the cryosections, explaining the higher abundance of 6 nm gold particles compared to 12 nm gold particles. Another noteworthy finding was the presence of TbRab5A and TbRab7 in the lysosomal lumen, suggesting their possible degradation (**Figure 8, A** and **B**).

In addition, the endosomal membranes were juxtaposed to the trans-Golgi in all Tokuyasu tomograms, further implying a role of the endosomal system in post-Golgi trafficking (**Figure 8, A** I and B III). In summary, our second 3D electron microscopy approach successfully visualized the continuous membrane system of the endosomal apparatus in *T. brucei* and represents the first utilization of the advanced 3D Tokuyasu technique in trypanosomes.

Discussion

Evolution has endowed African trypanosomes with a cellular multi-tool, the VSG-surface coat. Apart from exhibiting antigenic variation across hundreds of coat variants, the VSG proteins are attached to the cell surface through GPI-moieties, enabling their remarkable mobility. Exploiting this feature, the parasites evade early immune responses by clearing antibodies. This evasion process hinges upon the highly polarized nature of the trypanosome cell body, with exclusive endocytic uptake occurring at the posterior end, coupled with an exceptionally rapid membrane recycling rate. The prevailing model of the endosomal system, consisting of distinct compartments for early, late, and recycling endosomes, seems incompatible with the observed rapid turnover rates in *T. brucei*. Nevertheless, the parasite expresses the canonical Rab GTPases which serve as markers for these endosomal compartments, such as Rab5 (early), Rab7 (late), and Rab11 (recycling endosomes). To resolve this apparent contradiction, we performed a structure-function analysis of the trypanosome endosome apparatus.

3D electron tomography reconstructions, utilizing cargo uptake assays (**Figure 1**; Supplementary movie 1), revealed a complex network of endosomal structures in *T. brucei*. These compartments were characterized by interconnected fenestrated sheets, circular cisternae, and tubular structures, that formed a single intricate endosome. Our results shine a new light on transmission electron microscopic studies of the trypanosome endomembrane system (reviewed in Link et al., 2021). Based on 2D information the giant endosomal sheets had been interpreted as extended tubular structures, fenestrations as vesicles and the connective areas as irregularly shaped structures (Engstler et al., 2004; Grünfelder et al., 2003; Overath and Engstler, 2004).

In mammalian cells, tubular endosomes constitute a major part of the endosomal system. Tubules possess a higher surface area-to-volume ratio compared to vacuolar regions. As a result, they have been proposed to geometrically sort membrane-associated proteins over soluble cargo (Mayor et al., 1993). It is assumed that the carrier tubules, following detachment, transport their cargo either to the plasma membrane or to the recycling endosomes.

T. brucei lacks elongated tubulo-vesicular structures. Furthermore, our tomographic analysis did not reveal the conventional tubular carriers (reviewed in Chi et al., 2015). Instead, in these parasites, geometric sorting most likely occurs at the rims of flat, fenestrated sheets. A specific

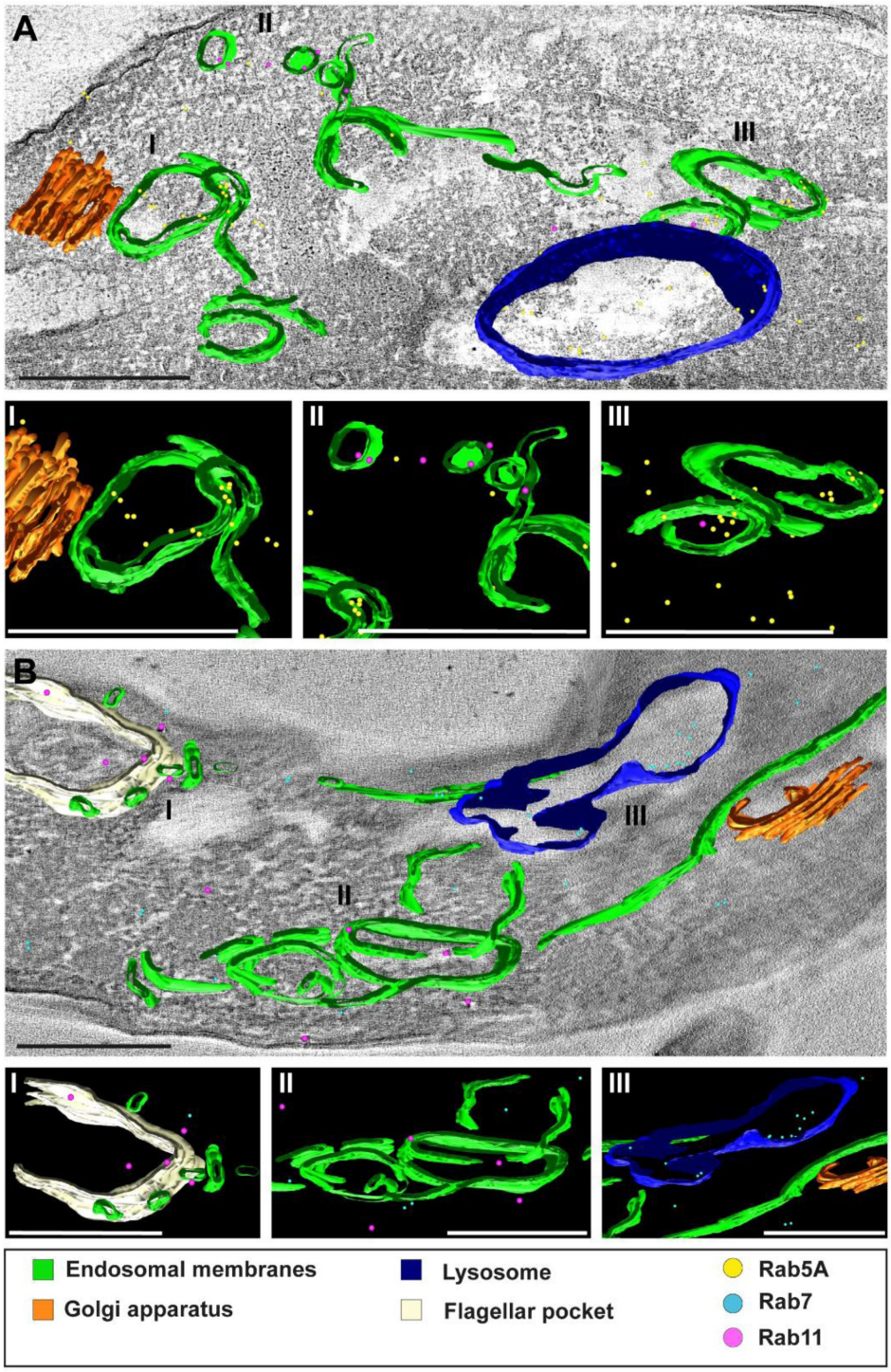

Figure 8.

3D Tokuyasu demonstrated continuous endosomal membranes in cryosections.

(A, B) Tomographic reconstruction of the endosomal apparatus. **(I – III)** Isolated view of different organelle structures. Cryosections (250 nm) were labelled with anti-TbRab antibodies and 6 or 12 nm gold-coupled secondary antibodies. Endosomes are shown in green, lysosomes in blue, the flagellar pocket in white, the Golgi apparatus in orange. Gold particles are indicated as coloured spheres; TbRab5A (yellow), TbRab7 (cyan) or TbRab11 (magenta). Scale bars: 500 nm. Movies corresponding to panel A and B can be found here: A) z-stack, 3D model; B) z-stack, 3D model. The provided tomograms serve as a representative sample among the 35 tomograms that were recorded.

class of clathrin-coated vesicles (CCV II) pinches off from these strongly curved membrane areas. They transport bulky fluid phase cargo and membrane protein complexes (such as VSG^{IgG}) to the lysosome (Engstler et al., 2004; Grünfelder et al., 2003).

The sorting mechanism into CCV II vesicles could be a purely physical process. Both the fenestrated sheets and circular cisternae exhibit the same inner width of about 35 nm. The VSG coat occupies 2 x 15 nm of this width, significantly limiting the available volume for fluid phase cargo. As the VSG concentration in the membrane increases, the bulky cargo is pushed towards the edges of the sheets, resulting in further membrane deformation that facilitates the recruitment of clathrin. The VSG is excluded from the CCV II and thus not transported to the lysosome. How this works mechanistically is unknown, however, it is tempting to speculate that the geometric sorting of larger cargo into the CCV II, sterically excludes VSG.

The electron tomographic analysis of the *T. brucei* endosome yielded compelling evidence of an extensive and interconnected membrane system. While this conclusion is supported by a substantial number of tomograms, the technique is not well suited for quantitative analyses.

Therefore, we conducted super-resolution microscopy and cargo uptake assays (**Figure 2** and S1). To analyse the full 3D volume of the cell, expansion microscopy was conducted (**Figure 2**). The visualised endosomal network looked like the elongated and circular structures found in the reconstruction of the electron tomograms (**Figure 1**). While the elongated structures could easily correspond to the fenestrated sheets (**Figure 2 A**), the circular structure (**Figure 2 A**, middle row, image III, arrow) nicely recapitulates the morphology of a circular cisternae (**Figure 1 C**). Interestingly, dividing cells (possessing two kinetoplasts and two flagellar pockets) always showed a fluorescence signal corresponding to the endosomal system juxtaposed only to the “old” flagellar pocket, indicating that the duplication of the endosomal network might occur *de novo* during the cell cycle. This is currently speculation and requires more in-depth analysis. The 3D presentation (**Figure 2 B**) confirmed the continuity of the endosomal membranes, which had been seen already in the electron tomography.

In contrast to *d*STORM or SIM, expansion microscopy (ExM) offers a selective perspective on the trypanosome endosomal system. To date, ExM has been effectively employed to visualize cell structures associated with the cytoskeleton or other stabilizing supports (Alonso, 2022; Amodeo et al., 2021; Gambarotto et al., 2019; Gorilak et al., 2021; Kalichava and Ochsenreiter, 2021). However, we could not find any published ExM images of endosomes. Our initial efforts to identify endosomal markers using ExM were also unsuccessful. Only when we added the inert fluid phase cargo dextran did the endosomes become clearly visible. This was likely due to the stabilizing effect of the cargo.

Having established that the endosomes in trypanosomes likely form a continuous cellular structure, our next inquiry was whether this would be evident in the simultaneous presence of the canonical marker proteins TbRab5A, TbRab7, and TbRab11. To define the region of interest in 3D immunofluorescence microscopy, we utilized the previously established fluorescent marker EP1::GFP (Engstler and Boshart, 2004), which stains the entire endosomal system. Maximum intensity projections (MIPs) of multichannel images indicated that the TbRabs were closely juxtaposed but in distinct endosomal compartments (**Figure 3 A**, upper row). This finding aligns with the results of a previously published quantitative colocalization analysis of TbRab5A and TbRab7 (Engstler et al., 2004). However, the presentation as 3D objects already implied an overlap between the different marker proteins. The present study now reveals that endosomal sheets can easily span over several micrometres, which fundamentally alters the interpretation of the light microscopy colocalization data. Thus, the seemingly separate structures could well be subdomains of the same membrane structure.

We therefore performed quantitative colocalization analyses with all marker combinations (**Figure 3**). The degree of colocalization was assessed by determining the percentage of overlap for the volume of one TbRab marker colocalized with another. Notably, TbRab5A and TbRab7 exhibited a significantly higher percentage of overlap (about 53 %) compared to the other marker combinations (**Figure 3 C**). An overlap of Rab5 and Rab7 has also been found in mammalian cells where it has been attributed to a temporary phenomenon during the maturation of early to late endosomes (Podinovskaia et al., 2021; Rink et al., 2005; van der Beek et al., 2021).

Interestingly, TbRab7 exhibited a higher degree of colocalization with TbRab11 (45 %) than TbRab5A showed with TbRab11 (35 %). This observation could indicate a functional polarization within the flagellar pocket. TbRab11 is known to decorate disk-shaped structures called exocytic carriers (EXCs), which transport the recycled VSG coat back to the cell surface. Boehm and colleagues (2017) report that in the flagellar pocket endocytic and exocytic sites are in close proximity but do not overlap. We further suggest that the fusion of EXCs with the flagellar pocket membrane and clathrin-mediated endocytosis take place on different sites of the pocket. This disparity explains the lower colocalization between TbRab11 and TbRab5A. It is worth noting that the mechanism by which Golgi-derived membrane and cargo are transported to the flagellar pocket in trypanosomes remains unclear. In our view, the most plausible scenario involves feeding into the rapid endocytic recycling pathway, which is further supported by the absence of tubular carriers as observed in mammals.

Quantitative colocalization analysis by 3D IF provides statistically valid results, however, has the obvious limitation that it lacks ultrastructural information. Therefore, we analysed the localization of the different TbRab proteins on cryo-electron micrographs. This finally proved that different TbRab markers can be found on the same membrane structures and argues against the existence of distinct early, late, and recycling endosomal compartments in *T. brucei* (**Figures 4**, **5** and **6**). An alternative explanation for the two marker proteins residing on the same membrane would the endosome maturation model, which has been proposed in mammals (Poteryaev et al., 2010; Rink et al., 2005; Stoorvogel et al., 1991). In short, early endosomes undergo maturation and transform into late endosomes through a series of changes. This maturation process involves the acquisition of new membrane proteins and enzymes that among others facilitate a decrease in the pH value. Ultimately, the late endosomes fuse with lysosomes, leading to cargo degradation (reviewed in Podinovskaia and Spang, 2018).

EM-cryosections provide high-resolution 2D information. To gain volume information, we resorted to an extremely demanding technique that combines ultrastructural 3D information with immunodetection. 3D Tokuyasu has not been applied to trypanosomes and the utilisation of 3D immunogold has not been used on endosomes in any system. The Tokuyasu tomograms clearly showed the connection of circular cisternae and sheet-like structures in 3D (**Figure 8**). The decoration with different endosomal marker proteins demonstrated the existence of functional subdomains within a giant endosomal membrane system convincingly, and finally offered an explanation to the fundamental question of how trypanosomes can combine endosomal functionality with very fast membrane recycling.

Our work has certainly raised more questions than it has answered. One puzzling aspect is the presence of extended sheet-like endosomal structures that display sparse or no labelling of TbRab proteins. This is particularly intriguing when considering the substantial membrane area covered by these sheets. It is tempting to speculate that the absence of canonical markers correlates with a lack of endosomal function. We postulate that these sheets represent “endosomal highways” that support fast flow of cargo by facilitated diffusion. This may allow for the efficient transport of VSG and fluid-phase cargo between distinct functional endosomal subdomains, which can be in close proximity or at a distance of microns apart. Consequently, the slow vesicular trafficking process in

trypanosomes could be limited to clathrin-coated vesicles, originating either from the flagellar pocket or the rims of fenestrated sheets and cisternae, as well as to Rab11-positive exocytic carriers.

Interestingly, we did not find any structural evidence of vesicular retrograde transport to the Golgi. Instead, the endosomal 'highways' extended throughout the posterior volume of the trypanosomes approaching the trans-Golgi interface. It is highly plausible that this region represents the convergence point where endocytic and biosynthetic membrane trafficking pathways merge. A comparable merging of endocytic and biosynthetic functions has been described for the TGN in plants. Different marker proteins for early and recycling endosomes were shown to be associated and/ or partially colocalized with the TGN suggesting its function in both secretory and endocytic pathways (reviewed in Minamino and Ueda, 2019). As we could not find structural evidence for the existence of a TGN we tentatively propose that trypanosomes may have shifted the central orchestrating function of the TGN as a sorting hub at the crossroads of biosynthetic and recycling pathways to the endosome. Although this is a speculative scenario, it is experimentally testable.

In summary, we confirmed the endosomal identity of the analysed membranes with the aid of cargo uptake assays (**Figure 1**, **2** and **7**), transgenic cell lines (**Figure 2** and **3**) as well as immuno labelling (**Figure 3** - **8**) combined with various light and electron microscopy methods. In the process, we ensured that all examined membranes belonged to the endosomal system and we did not, for example, mischaracterize ER membranes as endosomal membranes. All our results suggest that the endosomal apparatus consists of a continuous membrane system with TbRab5A, TbRab7 or TbRab11 positive subdomains that can be dynamically formed (**Figure 9**). Thus, the overall architecture of the trypanosome endosomes represents an adaptation that has facilitated the extreme speed of plasma membrane recycling observed in these organisms.

A partially continuous endosomal membrane structure has been proposed in the South American parasite *Trypanosoma cruzi* (Alcantara et al., 2018; Porto-Carreiro et al., 2000), however, no endosome markers were used in that study to corroborate their findings. In the single-celled parasite *Giardia*, the peripheral vesicles that constitute the endosomal organelles form an "interconnected network" (reviewed in Benchimol and de Souza, 2022), while the endosome-like compartment in *Toxoplasma* is likely involved in both endocytic and exocytic trafficking (reviewed in McGovern et al., 2021). In *Leishmania,* the endosomal system has not been fully characterized but seems to be under physical tension (reviewed in Ansari et al., 2022). Thus, parasitic protozoa might feature interesting variations of the common cell biological process of endocytosis. Furthermore, these variations might extend to many other organisms beyond the extensively studied, yet not entirely representative model organisms. The emergence of technologies such as CRISPR and single-cell analyses now enables the systematic exploration of the vast diversity of eukaryotic cells. Therefore, the systematic investigation of the phylogeny of cell biological inventions could be a logical next step.

Material and methods

Cell culture and cell lines

T. brucei bloodstream-form parasites (Lister strain 427, antigenic type MITat 1.2, clone 221) were cultured in HMI-9 medium (Hirumi and Hirumi, 1989) supplemented with 10 % heat-inactivated foetal calf serum (Sigma-Aldrich), 100 U/ml penicillin and 0.1 mg/ml streptomycin. The cells were maintained at 37 °C and 5 % CO_2 split at regular intervals to keep the population densities below 1 x 10^6 cells/ml. Population density was monitored using a Z2 Coulter Counter (Beckman Coulter). The monomorphic "13-90" parasites expressing the T7 RNA polymerase and tetracycline repressor were cultivated in the presence of 5 µg/ml hygromycin and 2.5 µg/ml G418 (Wirtz et al., 1999).

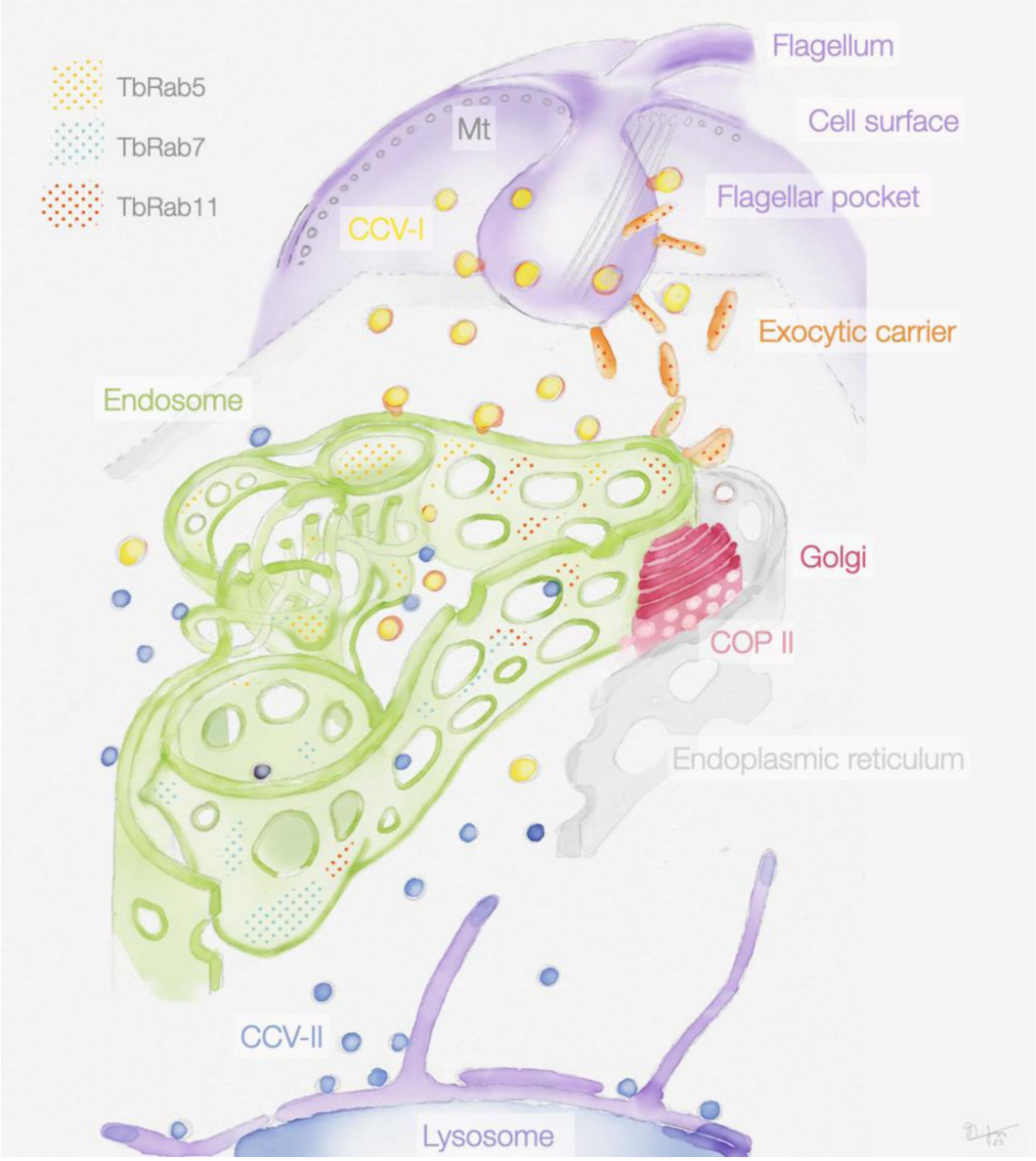

Figure 9.

Schematic representation of the endosomal system in *T. brucei*.

The endosome is marked by the presence of small GTPases of the Rab family: Rab5A (yellow dots), Rab7 (cyan dots), and Rab11 (red dots). Class I clathrin-coated vesicles (CCV-I), class II clathrin-coated vesicles (CCV-II), vesicles coated with coat protein (COP) II.

The transgenic bloodstream form “2T1” cells which constitutively express a T7 RNA polymerase and tetracycline repressor were cultivated in the presence of 2.5 µg/ml phleomycin and 1 µg/ml puromycin (Alsford et al., 2005). The RNAi cell lines (RNAi-TbRab5A, RNAi-TbRab7, RNAi-TbRab11) were based on the 2T1 cell line and cultivated in the presence of 5 µg/ml hygromycin and 2.5 µg/ml phleomycin. The transgenic EP1::GFP cells were based on MITat1.2 expressing wild type cells and cultivated in the presence of 5 µg/ml hygromycin and 15 µg/ml G418 (Engstler and Boshart, 2004). The transgenic single marker (SM) cell line (Wirtz et al., 1999) which constitutively express a T7 RNA polymerase and tetracycline repressor were cultivated in the presence of 2.5 µg/ml G418. The EP1::Halo tagged cell line was based on SM cells and was cultivated in the presence of 2.5 µg/ml phleomycin and 2.5 µg/ml G418.

Generation of RNAi cell lines

The RNAi target sequences were selected by entering the target gene ORF into the RNAit webapp (Redmond et al., 2003). The selected primer pairs flanked the base pairs 29 – 614 (TbRab5A), 134 – 630 (TbRab7) or 67 – 496 (TbRab11) and encoded the attB-sequence at the 5’ end for the ligation into the pGL2084 plasmid (Jones et al., 2014). The plasmids were linearized with AscI and 10 µg were transfected into 3 x 10^7 mid-log phase bloodstream 2T1 cells (Alsford et al., 2005) using Amaxa Basic Parasite Nucleofector Solution 1 using the X-001 program of an Amaxa Nucleofector II (Lonza, Switzerland). Clones were selected by growth in medium containing phleomycin (2.5 µg/ml) and hygromycin (5 µg/ml).

Generation of EP1::Halo cell line

The insert for the EP1::HaloTag cell lines was generated in resemblance to the GFP::EP1 cell line from Engstler and Boshart (2004). For this, the Halo tag was inserted in between the N-terminal EP1 globular domain and the C-terminal EP1 stalk domain. The three fragments (EP1 globular domain, Halotag, EP1 stalk domain) were amplified using PCR. For the EP1 fragments, the GFP::EP1 plasmid was used (Engstler and Boshart, 2004). While amplifying the globular domain, an internal BamHI restriction site was removed by silent point mutation. The Halo tag sequence was amplified from the pFC20A (HaloTag®) T7 SP6 Flexi® vector (Promega, USA). All amplified fragments were then combined using Gibson assembly (Gibson assembly cloning kit, NEB) with 20 base pair overhangs. This construct was cloned into pJet1.2blunt and later excised using HindIII and BamHI for ligation into the pLew100v5 expression vector (Wirtz et al., 1999). For transfection of the parental, SM cell line, 10 µg of the NotI linearized plasmid was transfected. Clones were selected by growth in medium containing phleomycin (2.5 µg/ml) and G418 (2.5 µg/ml). Primers used: forward primer globular domain (AGTAAAATTCACAAGCTTGG ATGGCACCTCGTTCCCTTTATCTGCTCGCTGTTCTTCTGTTCAGCGCGAACCTCTTC GCTGGCGTGGGATTTGCCGCAGCCGCTGAAGGACCAGAAGACA), reverse primer globular domain (CCGATTTCTGCCAT TCTAGAGGTGGCGACCGGCCGGTGAATCCCGCCGACCTTGGTTCCCTTCTCGCCTT TGCCTTTGCCTCCCTTAGTAAGACCCTTGTCTTCTGGTCCTTCAGCGGCT), forward primer Halo tag, (TCTAGA ATGGCAGAAATCGGTACTGGCTTTCCATTCG), reverse primer Halo tag (TCAGTGCCATTGGTATCGTCCTTAATT AACCCGGAAATCTCCAGAGTAGACAGCC), forward primer stalk domain (TTAATTAA G GACGATACCAATGGCACTGACC), reverse primer stalk domain (AAAAGCCAACTAAATGGGCA GGATCC TTAGAATGCGGCAACGAGAGC).

Growth curves

Cells were seeded with a starting concentration below 1 x 10^6 cells/ml in a volume of 10 ml and divided into two 2 ml aliquots in separate wells of a 24-well plate. Tetracycline was added to a final concentration of 1 µg/ml in one well to induce RNAi or EP1::Halo expression. The population density of the non-induced and induced cells was determined every 24 h over a time course of 96 h, using a Z2 Coulter Counter (Beckman Coulter). Depletion of the target protein was confirmed by immunoblotting of whole-cell lysates (Supplements 2).

Cargo uptake

Per assay the same number of cells (1 x 10^7 for light microscopy, 1 x 10^8 for electron microscopy) were harvested by centrifugation (1500 x *g*, 10 min, 4 °C). After that, cells were washed with 1 ml TDB (5 mM KCl, 80 mM NaCl, 1mM $MgSO_4$, 20 mM Na_2HPO_4, 2 mM NaH_2PO_4, 20 mM glucose, pH 7.6), harvested by centrifugation (1500 x *g*, 2 min, 4 °C) and the supernatant was discarded. Next, the cells were resuspended in 100 µl TDB and incubated with either dextran-Alexa488 (light microscopy), transferrin-gold conjugates or BSA-gold conjugates (electron microscopy) for 15 min at 37 °C or HRP/ferritin for 5 min at 37 °C (electron microscopy). The final concentration of both dextran (ThermoFisher cat. number: D22910) and HRP (horseradish peroxidase type II, Sigma) was 10 mg/ml. The final concentration of ferritin (horse spleen ferritin, type I, Sigma) was 50 mg/ml. Transferrin-gold (Cytodiagnostics) or BSA-gold (Alexa555-BSA-Au, UMC Utrecht) were added to a final OD = 5. The uptake reactions were stopped by adding 1 ml of the corresponding fixatives (4 % formaldehyde and 0.2 % glutaraldehyde for the dextran uptake, 2 % formaldehyde and 0.2 % glutaraldehyde for BSA and transferrin uptake, 2.5 % glutaraldehyde for HRP uptake, 2 % formaldehyde and 1 % glutaraldehyde for ferritin uptake). Cells were fixed for 20 min on ice followed by 30 min at RT (for dextran uptake), 1 hour at RT (for HRP and ferritin) or 2 hours at RT (for BSA and transferrin uptake). Following this, cells were treated either as described in the immunofluorescence section or as explained in the sample embedding and immuno-electron microscopy section.

EP1::Halo cell labelling

Cells were harvested (1400 x *g*, 10 min, 37 °C) and washed in 1 ml TDB. The cell pellet was resuspended in 100 µl fresh TDB and HaloTag ligand (either in-house labelled Alexa647 ligand or Halo-Tetramethylrhodamine (TMR, Promega, USA) was added to a final concentration of 500 nM (Alexa647) or 5 nM (TMR). The labelling reaction was performed for 15 min at 37 °C and stopped by the addition of 4 % formaldehyde in PBS.

Immunofluorescence

Cells were harvested (1400 x *g*, 10 min, 37 °C), washed in ice-cold TDB, and fixed with 4% formaldehyde overnight (4 °C) or for 1 hour at RT. Fixed samples were washed in 1 ml PBS, harvested (1400 x *g*, 90 sec, RT) and 1 x 10^6 cells were added to each Ø 12 mm coverslip coated with 0.01 % poly-L-lysine (> 20 min, RT). The cells were attached to the coverslips by centrifugation (750 x *g*, 1 min, RT) and attachment was confirmed visually. The attached cells were then permeabilized in 0.25 % Triton X-100 in PBS (5 min, RT) and blocked in 3 % (w/v) BSA in PBS (30 min, RT). Sequentially, coverslips were incubated with primary antibodies (1 h, RT), washed with PBS (3 x 5 min), and incubated once more with secondary antibodies (1 h, RT, in the dark). Finally, samples were washed in PBS (3 x 5 min), rinsed in ddH_2O, carefully dried, and mounted on glass slides using ProLong™ Diamond Antifade (Life Technologies). Antibodies were diluted in 1 % (w/v) BSA in PBS as follows: rat anti-TbRab5A 1:250, guinea pig anti-TbRab7 1:250, rabbit anti-TbRab11 1:250, goat anti-rat conjugated with Alexa Fluor 647 1:500, goat anti-guinea pig conjugated with CF568 1:500, goat anti-rabbit conjugated with Alexa Fluor 405 1:500.

Expansion microscopy

The proExM method was performed as described in (Tillberg et al., 2016) with some modifications. Approximately 1 x 10^7 cells were harvested by centrifugation (1500 x *g*, 10 min, 4 °C), then washed with 1 ml TDB, harvested by centrifugation (1500 x *g*, 2 min, 4 °C) again, and the supernatant was discarded. Next, the cells were resuspended in 100 µl TDB and incubated with dextran-Alexa488 for 15 min at 37 °C. The final concentration of dextran (ThermoFisher cat. number: D22910) was 10 mg/ml. The reaction was stopped by adding 1 ml 4 % formaldehyde and 0.2 % glutaraldehyde in PBS. Cells were fixed for 20 min on ice followed by 30 min at RT. After the fixation, cells were adhered to 12 mm coverslips. For anchoring of proteins, a solution of 5 mg AcX (A20700, Invitrogen), dissolved in freshly opened 500 µl anhydrous DMSO (D12345, Invitrogen),

was prepared. A 100 µl drop of AcX 1:100 in PBS was placed on parafilm in a humidity chamber, the coverslips were inverted and incubated at room temperature for 16 hours. Coverslips were returned to a 24-well plate, washed twice for 5 minutes with PBS and stored in the fridge until the end of the day. For gelation, gelling solution was made mixing 100 µl monomer solution with 0.5 µl 10 % (v/v) APS and 0.5 µl TEMED, vortexed and used straight away. A volume of 50 µl was placed on a piece of parafilm in a humidity chamber and the coverslips were inverted and incubated at 37 °C for one hour. Monomer solution was prepared with sodium acrylate 8.6 % (w/v) (408220, Sigma), acrylamid 2.5 % (w/v), N-N'-methylenebisacrylamide 1.5 % (w/v) (M7279, Sigma) and NaCl 11.7 % (w/v) (AM9760G, Ambion) in PBS. Sodium acrylate stock solution 33 % (w/v) was prepared by dissolving 1.9 g in 5 ml of ddH_2O, 0.2 mm-filtered and used freshly. After polymerization, coverslips with the gel stuck to it were transferred to a 6-well plate with 1 ml of digestion solution (0.5 % Triton X100, 1 mM EDTA, pH 8 (AM9260G, Ambion), 50 mM Tris, pH 8 (AM9855G, Ambion) and 1 M NaCl (AM9760G, Ambion) freshly supplemented with 10 U/ ml proteinase K (P8107S, New England Biolabs). Plates were slightly tilted to ensure the coverslip was completely covered and incubated at room temperature overnight. The next day, gels were detached from the coverslips and transferred to a Petri dish. After three rounds of expansion with 20 ml ddH_2O for 30 minutes each, gels were mounted in a poly-D-lysine coated imaging chamber (Nunc 155360 Lab-Tek II Chambered Coverglass with Cover, No. 1.5 Borosilicate Sterile) and imaged using a DMi8 widefield microscope.

Fluorescence microscopy

Images were acquired using a DMi8 widefield microscope (Thunder Imager, Leica Microsystems, Germany) with a HCX PL APO CS objective (100 x oil-immersion, NA 1.4, working distance 90 µm) and Type F Immersion Oil (refractive index = 1.518, Leica Microsystems, Germany). The microscope was operated using LAS-X software (Leica). Samples were illuminated with an LED8 light source (Leica) and 50 % illumination power. Excitation light was selected by using following filter sets: 391/32 nm; 479/33 nm; 554/24 nm; 638/31 nm (Leica Microsystems, Germany). Emitted light was collected at 435/30 nm (DAPI and Alexa Fluor 405), 519/25 nm (Dextran-Alexa Fluor 488 and GFP), 594/32 nm (CF568 and TMR) and 669 nm (Alexa Fluor 647), respectively. The individual exposure times were as follows: DAPI, Alexa Fluor 405, CF568, Alexa Fluor 647 = 200 ms; GFP = 500 ms; Dextran-Alexa Fluor 488 = 2 s; TMR = 2 s. Differential interference contrast (DIC) was used to visualise cell morphology. 3D recording of each field of view was obtained using 48 z-slices (step size = 0.21 µm). Fields of view were selected based on DIC to subjectively select for areas containing enough cells and blind the user to the fluorescence signal of the protein markers of interest. Images were captured using a Leica K5 sCMOS camera (pixel size 6.5 µm). The LAS-X/ Thunder integrated instant computational clearing (ICC) algorithm was used to remove background signal, using a minimal structure size of 338 nm.

Colocalization analysis

Widefield microscopy images were deconvolved using Huygens Essential version 21.10 (Scientific Volume Imaging B.V., Hilversum, Netherlands) and analyzed with IMARIS (9.9.1, Oxford Instruments). In brief, surfaces were rendered for the EP1 signal, and checked manually for accurate posterior localization in morphologically intact cells. These EP1 surfaces were used to define the ROI for colocalization analysis. The automatic thresholding function (Costes et al., 2004) was used to ensure objective thresholding for the colocalization analysis of the different TbRab marker protein combinations.

*d*STORM imaging

Direct stochastic optical reconstruction (*d*STORM) imaging was performed on an inverted wide-field microscope (Olympus, IX-71). HaloTag-Ligand Alexa Fluor 647 was excited by a 641 nm diode laser (Topica, iBeam smart 640-S), a 405 nm diode laser (Coherent, Cube 405-100C) was used for DAPI excitation. Both Lasers were spectrally cleaned with cleanup filters (Chroma, laser clean up

filter 640/10 & 405/20) and focused on the back focal plane of a 60x oil-immersion objective (Olympus, 60x NA 1.45). Emission light was separated from excitation light using a dichroic beam splitter (Semrock, FF410/504/583/669) and further spectrally filtered by a long-pass filter (Semrock, 647 nm RazorEdge). Images were recorded on an EM-CCD camera chip (Andor, iXon DU-897) with a measured pixel size of 134 nm. *d*STORM imaging was performed in a buffer of 100 mM MEA (Sigma-Aldrich, #M6500) in PBS at pH 7.4. Time series of 15 000 frames at an exposure time of 20 ms were captured while irradiating the sample by highly inclined laminated optical sheet (HILO) illumination with an intensity of approx. 2 kW cm^{-2}. Super-resolved images were reconstructed with rapidSTORM 3.3 (Wolter et al., 2012) and further processed for illustrations in Fiji. Widefield images of transmitted light and DAPI staining were captured after *d*STORM. For illustrations, the scale of the widefield images was matched to the super-resolved *d*STORM images.

SIM imaging

Structured Illumination imaging was performed using a Zeiss Elyra 7 lattice SIM equipped with a 63x C-Apochromat 63x/1.20 W (Zeiss) water immersion objective, four excitation lasers (405 nm diode, 488 nm OPSL, 561 nm OPSL, and 642 nm diode laser) and two sCMOS (PCO, pco.edge 4.2) cameras. Four-fold expanded gels were transferred onto PDL coated single well chamber slides (CellVis, #C1-1.5H-N). For excitation of DAPI the 405 nm laser diode was set to 10 % output power, for excitation of Dextran-Alexa488 the 488 nm laser to 20 %. A respective exposure time of 100 ms and 200 ms was set for the two channels. Z-stacks were captured in 3D Leap mode with optimal step intervals and appropriate filter sets (BP 420-480 + LP 655 and BP 495-550 + BP 570-620 for the DAPI- and 488-channel, respectively). SIM imaging was performed by capturing 13 phase-shifts of the lattice SIM pattern per slice. Super-resolved images are processed in ZEN 3.0 SR FP2 (black) (Zeiss, Version 16.0.10.306) with SIM and SIM² processing modules.

Sample embedding and preparation for electron microscopy

For Tokuyasu immuno-EM, sample preparation and sectioning were performed as previously described (Engstler et al., 2004; Grünfelder et al., 2003; Möbius and Posthuma, 2019; Slot and Geuze, 2007). In short, 1 x 10^8 cells were harvested (1500 x *g*, 10 min, 37 °C) and washed with 1 ml TDB. Cells were fixed by addition of 4 % formaldehyde and 0.4 % glutaraldehyde in 0.2 M PHEM buffer (120 mM PIPES, 50 mM HEPES, 4 mM $MgCl_2$, 20 mM EGTA adjusted to pH 6.9 with 1 M NaOH) 1:1 to TDB. After 5 min the fixatives were replaced with 2 % formaldehyde and 0.2 % glutaraldehyde in 0.1 M PHEM for 2 hours at RT. Fixatives were removed by washing with 1 ml TDB and quenched with PBS + 0.15 % (w/v) glycine. Cells were pelleted and resuspended in 200 µl 12 % (w/v) gelatine (Rousselot 250 LP30) in 0.1 M PHEM at 37 °C and pelleted again. The pellets were solidified on ice, cut into smaller blocks, and infused with 2.3 M sucrose in 0.1 M PHEM overnight at 4 °C. The blocks were mounted on metal pins and stored in liquid nitrogen. The gelatine-embedded cells were cryosectioned to 55 nm or 250 nm thick sections at −120 °C or −100 °C, respectively, with a DiATOME diamond knife in a Leica ultracut cryomicrotome (UC7). Sections were collected and deposited on formvar- and carbon-coated grids using 2.3 M sucrose and 1.8 % (v/v) methylcellulose (MC; Sigma M6385 25 centipoises) mixed 1:1.

For Epon embedding, sample preparation and sectioning were performed as previously described (Langreth and Balber, 1975; Webster, 1989). In short, chemically fixed cells were pelleted (1500 x *g*, 10 min, RT) and washed 6 x in 0.12 M sucrose, 0.1 M cacodylate, pH 7.4. They were postfixed in 1 % (w/v) osmium tetroxide, stained *en bloc* in 1 % (w/v) uranyl acetate in 50 mM sodium maleate buffer (pH 5.1), dehydrated with ethanol and embedded at 60 °C in epoxy resin. Cells incubated with HRP were treated, in suspension, with diaminobenzidine (DAB) in 50 mM Tris-HCl (pH 7.6) containing 0.01 % (v/v) osmium tetroxide for 5 min prior to postfixation with 1 % osmium tetroxide. The epon-embedded cells were sectioned to 250 nm thick sections at RT.

Immuno-electron microscopy

Grids with sections facing down were incubated in a 24-well plate with 2 ml PBS at 37 °C for 30 – 60 min to remove gelatine, 2.3 M sucrose and 1.8 % MC mixture. Afterwards, the grids were washed on ~ 100 µl drops of PBS + 0.15 % (w/v) glycine and PBS on parafilm at RT (both 3 x 5 min). The standard volume for all non-antibody related steps was100 µl. Next, blocking was performed in PBS + 0.1 % (v/v) acetylated BSA (BSA-c, Aurion) + 0.5 % (w/v) cold fish-skin gelatine (FSG, Sigma) for 30 min. The following primary antibody incubation was done for 1 – 2 hours in PBS + 0.1 % BSA-c + 0.5 % FSG. The used antibody dilutions were rat anti-TbRab5A 1:50, guinea pig anti-TbRab7 1:50, rabbit anti-TbRab11 1:25, and rabbit anti-VSG 1:50. After that, grids were washed 5 x 5 min with PBS + 0.1 % BSA-c + 0.5 % FSG and incubated with corresponding gold coupled secondary antibodies for 1 – 2 hours (diluted 1:10 in PBS + 0.1 % BSA-c + 0.5 % FSG). Further washing steps with PBS + 0.1 % BSA-c + 0.5 % FSG (3 x 5 min) and PBS (3 x 5 min) followed before all remaining antibodies were fixed with 1.25 % glutaraldehyde for 5 min at RT. After three washing steps with ddH_2O to remove phosphate from the grids, sample contrast was increased by 5 min incubation on 2 % (w/v) uranyl acetate (UA) in water (pH 7) and 7 min incubation on 1.8 % (v/v) MC/ 0.3 % (w/v) UA in water (pH 4) (both on ice). Grids were retrieved with a metal ring and excess MC/UA was removed with filter paper. Grids were dried for at least 30 min at RT in the metal ring.

Electron Microscopes

JEOL JEM-2100 transmission electron microscope (TEM) operated at 200 kV with camera system: TVIPS F416 4k x 4k.

JEOL JEM-1400 Flash scanning transmission electron microscope (STEM) operated at 120 kV with camera system: Matataki Flash 2k x 2k.

FEI Tecnai TF30 transmission electron microscope (TEM) operated at 300kV with camera system: Gatan US4000 4k x 4k CCD.

The software Serial EM was used for tilt series acquisitions of electron tomograms. The subsequent reconstruction and segmentation were done using the IMOD software package (Kremer et al., 1996). For 2D electron micrographs pseudo colouring and highlighting was done using Adobe Illustrator 2022.

Immunoblotting

Trypanosomes were resuspended and lysed in protein sample buffer (60 mM Tris-HCl, pH 6.8, 2 % (w/v) SDS, 10 % (v/v) glycerol, 0.002 % (w/v) bromophenol blue, 1 % (v/v) β-mercaptoethanol) to yield equivalents of 2 x 10^5 cells/µl. For quantification of TbRab proteins by Western Blot 20 µl of the protein sample was resolved on 12.5 % SDS-PAGE gels and transferred onto nitrocellulose membrane. The membranes were blocked for 1 h at room temperature with 5 % (w/v) milk powder in PBS. Next, the membranes were incubated in polyclonal primary antibodies diluted in PBS containing 1 % (w/v) powdered milk and 0.1 % (v/v) Tween 20, anti-TbRab 1:5000 and monoclonal mouse anti-TbPFR (L13D6) 1:20 (Kohl et al., 1999). After wash steps, the membranes were incubated in IRDye 800 CW (Li-Cor) labelled either goat anti-rat, donkey anti-guinea pig, or donkey anti-rabbit and IRDye 680 LT (Li-Cor) labelled goat anti-mouse secondary antibodies diluted 1:10,000 in PBS containing 1 % (w/v) milk powder and 0.1 % (v/v) Tween 20. Images were acquired and quantified with the Li-Cor Odyssey system.

Recombinant protein expression and purification for antibody generation

The TbRab5A (Tb927.10.12960), TbRab7 (Tb927.9.11000), TbRab11 (Tb927.8.4330) open reading frames were amplified from *Trypanosoma brucei brucei* strain Lister 427 genomic DNA by PCR. The PCR product was digested with NdeI and XhoI restriction enzymes and ligated into the pET21-

a expression vector, which encodes an N-terminal His6 tag. The plasmid was used to perform a chemical transformation into *E. coli* strain Rosetta II (DE3) pLysS. Individual colonies were subsequently grown at 37 °C in presence of 100 µg/ml ampicillin to an OD600 of ~ 0.8. Recombinant protein expression was induced by the addition of 50 µM IPTG and the cells were incubated for 4 h at 37 °C with shaking. Cells were harvested by centrifugation (3000 x *g*, 10 min, 4 °C). The pellet was resuspended in 10 ml lysis buffer (100 mM NaH_2PO_4, 10 mM Tris/ HCl, 8M Urea, pH 8.0) and incubated for 1 h at RT on. Final lysis was then achieved with sonication on ice, using 6 cycles for 10 s with MiniTip step 7 (Sonifier, B-12, Branson Ultrasonics). Lysates were clarified by centrifugation (10,000 x *g*, 30 min, RT) and incubated for 1 hour with Ni-NTA His bind resin (Merck) rolling at RT. Afterwards, the resin was transferred to a HiTrap column (GE healthcare) and washed with 30 ml lysis buffer and 30 ml buffer B (100 mM NaH_2PO_4, 10 mM Tris/ HCl, 8 M Urea, pH 6.3). Next, the bound proteins were eluted with 1 x 2 ml buffer C (100 mM NaH_2PO_4, 10 mM Tris/ HCl, 8 M Urea pH, 5.9), 1 x 2ml buffer D (100 mM NaH_2PO_4, 10 mM Tris/ HCl, 8M Urea pH 4.5) and 1 x 2 ml buffer E (100 mM NaH_2PO_4, 10 mM Tris/ HCl, 8 M Urea, pH 4.5 + 250 mM imidazole). All elution's were then separately dialysed overnight against a 20 mM phosphate buffer (2.7 mM Na_2HPO_4, 17.3 mM NaH_2PO_4) at 4 °C. The purification success was validated by 15 % SDS-PAGE and proteins were sent to different companies for antibody generation.

Antibody generation

Recombinant full-size proteins were used to immunise different animals (Pineda, Berlin, Germany; Davids Biotechnology, Regensburg, Germany; Eurogentec, Seraing, Belgium). The resulting antisera were affinity purified against the immobilised recombinant protein. The resulting antisera from two rats (anti-TbRab5A) showed no need for affinity purification. All antibodies were validated for selectivity through immunoblots of the corresponding RNAi cell line (Supplementary 2).

HaloTag ligand labelling

HaloTag-Ligand-Amine (Promega, #P6741) was reconstituted in DMF (Sigma-Aldrich, #70547) to a concentration of 10 g/l. 250 µg HaloTag-Ligand Amine was conjugated to Alexa Fluor 647-NHS (Thermofisher, #A20006) by adding 150 µg of NHS-dye from a 10 g/l stock solution in DMF. The total reaction volume was adjusted to 120 µl with DMF, then DIPEA Base (Sigma-Aldrich, #387649) was added at 1:100. The reaction was incubated under gentle agitation and protected from light at room temperature for three hours. The reaction mixture was purified by reverse-phase high performance liquid chromatography (HPLC, Jasco) using a biphenyl column (Kinetex, #00F-4622-E0) with a solvent gradient of 0-60 % (v/v) acetonitrile (Sigma-Aldrich, #34851) in 0.1 % TFA (Sigma-Aldrich, #T6508) in water run over 30 min. Collected product fractions were dried in a speed-vac (Thermofisher, #SPD111V) and dissolved in DMSO.

Acknowledgements

We thank the Cell Microscopy Core of UMC Utrecht for their workshop "Cryosectioning and immuno-electron microscopy" and the opportunity to learn the Tokuyasu technique. Manfred Alsheimer provided protocols and advice with recombinant protein expression and antibody generation. Daniela Bunsen and Claudia Gehring-Höhn provided help with the EM benchwork and assistance with the electron microscope. Bernardo Gabiatti, Janna Eilts, Marcel Rühling and Tobias Kunz provided protocols and advice on expansion microscopy. We are grateful to Brooke Morriswood for essential discussions. We express our gratitude to the eLife reviewers for dedicating their time and effort to evaluate the manuscript. We sincerely value all the insightful comments and suggestions, particularly those related to obtaining tomograms of unprocessed cells for use as a control. These recommendations played a crucial role in enhancing the overall quality of the manuscript.

Funding

ME was supported by DFG grants EN305, SPP1726 (Microswimmers—From Single Particle Motion to Collective Behaviour), GIF grant I-473-416.13/2018 (Effect of extracellular *Trypanosoma brucei* vesicles on collective and social parasite motility and development in the tsetse fly) and GRK2157 (3D Tissue Models to Study Microbial Infections by Obligate Human Pathogens), the EU ITN Physics of Motility, and the BMBF NUM Organo-Strat. ME is a member of the Wilhelm Conrad Röntgen Center for Complex Material Systems (RCCM). The transmission electron microscopes in Würzburg were funded by the Deutsche Forschungsgemeinschaft (DFG, German Research Foundation) – 426173797 (INST 93/1003-1 FUGG) and 218894163. AB was supported by the Brazilian agency CAPES (program: CAPES/DAAD—Call No. 22/2018; process 88881.199683/2018-01). MJ was supported by GRK2157 and the European Research Council (ERC) under the European Union's Horizon 2020 research and innovation programme (grant agreement No 835102) awarded to MS.

References

1. Ackers J.P., Dhir V., Field M.C. (2005) **A bioinformatic analysis of the RAB genes of Trypanosoma brucei** *Mol Biochem Parasitol* **141**:89–97

2. Alcantara C.L., de Souza W., da Cunha E.S.N.L. (2018) **Tridimensional Electron Microscopy Analysis of the Early Endosomes and Endocytic Traffic in Trypanosoma cruzi Epimastigotes** *Protist* **169**:887–910

3. Allen C.L., Goulding D., Field M.C. (2003) **Clathrin-mediated endocytosis is essential in Trypanosoma brucei** *EMBO J* **22**:4991–5002

4. Alonso V.L. (2022) **Ultrastructure Expansion Microscopy (U-ExM) in Trypanosoma cruzi: localization of tubulin isoforms and isotypes** *Parasitology Research* **121**:3019–3024

5. Alsford S., Kawahara T., Glover L., Horn D. (2005) **Tagging a T. brucei RRNA locus improves stable transfection efficiency and circumvents inducible expression position effects** *Mol Biochem Parasitol* **144**:142–148

6. Amodeo S., Kalichava A., Fradera-Sola A., Bertiaux-Lequoy E., Guichard P., Butter F., Ochsenreiter T. (2021) **Characterization of the novel mitochondrial genome segregation factor TAP110 in Trypanosoma brucei** *Journal of Cell Science* **134**

7. Ansari I., Basak R., Mukhopadhyay A. (2022) **Hemoglobin Endocytosis and Intracellular Trafficking: A Novel Way of Heme Acquisition by Leishmania** *Pathogens* **11**

8. Bartossek T. *et al.* (2017) **Structural basis for the shielding function of the dynamic trypanosome variant surface glycoprotein coat** *Nat Microbiol* **2**:1523–1532

9. Becker M., Aitcheson N., Byles E., Wickstead B., Louis E., Rudenko G. (2004) **Isolation of the repertoire of VSG expression site containing telomeres of Trypanosoma brucei 427 using transformation-associated recombination in yeast** *Genome Res* **14**:2319–2329

10. Benchimol M., de Souza W. (2022) **Giardia intestinalis and its endomembrane system** *Journal of Eukaryotic Microbiology* **69**

11. Boehm C.M., Obado S., Gadelha C., Kaupisch A., Manna P.T., Gould G.W., Munson M., Chait B.T., Rout M.P., Field M.C. (2017) **The Trypanosome Exocyst: A Conserved Structure Revealing a New Role in Endocytosis** *PLoS Pathog* **13**

12. Borges A.R., Link F., Engstler M., Jones N.G. (2021) **The Glycosylphosphatidylinositol Anchor: A Linchpin for Cell Surface Versatility of Trypanosomatids** *Frontiers in Cell and Developmental Biology* **9**

13. Burki F., Roger A.J., Brown M.W., Simpson A.G.B. (2020) **The New Tree of Eukaryotes** *Trends in Ecology & Evolution* **35**:43–55

14. Chaves I., Rudenko G., Dirks-Mulder A., Cross M., Borst P. (1999) **Control of variant surface glycoprotein gene-expression sites in Trypanosoma brucei** *EMBO J* **18**:4846–4855

15. Chen F., Tillberg P.W., Boyden E.S. (2015) **Optical imaging. Expansion microscopy** *Science* **347**:543–548

16. Chi R.J., Harrison M.S., Burd C.G. (2015) **Biogenesis of endosome-derived transport carriers** *Cell Mol Life Sci* **72**:3441–3455

17. Costes S.V., Daelemans D., Cho E.H., Dobbin Z., Pavlakis G., Lockett S. (2004) **Automatic and quantitative measurement of protein-protein colocalization in live cells** *Biophys J* **86**:3993–4003

18. Cross G.A. (1975) **Identification, purification and properties of clone-specific glycoprotein antigens constituting the surface coat of Trypanosoma brucei** *Parasitology* **71**:393–417

19. Engstler M., Boshart M. (2004) **Cold shock and regulation of surface protein trafficking convey sensitization to inducers of stage differentiation in Trypanosoma brucei** *Genes Dev* **18**:2798–2811

20. Engstler M., Pfohl T., Herminghaus S., Boshart M., Wiegertjes G., Heddergott N., Overath P. (2007) **Hydrodynamic flow-mediated protein sorting on the cell surface of trypanosomes** *Cell* **131**:505–515

21. Engstler M., Thilo L., Weise F., Grunfelder C.G., Schwarz H., Boshart M., Overath P. (2004) **Kinetics of endocytosis and recycling of the GPI-anchored variant surface glycoprotein in Trypanosoma brucei** *J Cell Sci* **117**:1105–1115

22. Field H., Farjah M., Pal A., Gull K., Field M.C. (1998) **Complexity of trypanosomatid endocytosis pathways revealed by Rab4 and Rab5 isoforms in Trypanosoma brucei** *J Biol Chem* **273**:32102–32110

23. Gambarotto D., Zwettler F.U., Le Guennec M., Schmidt-Cernohorska M., Fortun D., Borgers S., Heine J., Schloetel J.-G., Reuss M., Unser M. (2019) **Imaging cellular ultrastructures using expansion microscopy (U-ExM)** *Nature Methods* **16**:71–74

24. Gorilak P., Pružincová M., Vachova H., Olšinová M., Schmidt Cernohorska M., Varga V. (2021) **Expansion microscopy facilitates quantitative super-resolution studies of cytoskeletal structures in kinetoplastid parasites** *Open Biology* **11**

25. Grünfelder C.G., Engstler M., Weise F., Schwarz H., Stierhof Y.D., Morgan G.W., Field M.C., Overath P. (2003) **Endocytosis of a glycosylphosphatidylinositol-anchored protein via clathrin-coated vesicles, sorting by default in endosomes, and exocytosis via RAB11-positive carriers** *Mol Biol Cell* **14**:2029–2040

26. Gull K. (2003) **Host–parasite interactions and trypanosome morphogenesis: a flagellar pocketful of goodies** *Current Opinion in Microbiology* **6**:365–370

27. Hall B.S., Smith E., Langer W., Jacobs L.A., Goulding D., Field M.C. (2005) **Developmental variation in Rab11-dependent trafficking in Trypanosoma brucei** *Eukaryot Cell* **4**:971–980

28. Hartel A.J., Glogger M., Jones N.G., Abuillan W., Batram C., Hermann A., Fenz S.F., Tanaka M., Engstler M. (2016) **N-glycosylation enables high lateral mobility of GPI-anchored proteins at a molecular crowding threshold** *Nat Commun* **7**

29. Heilemann M., van de Linde S., Schuttpelz M., Kasper R., Seefeldt B., Mukherjee A., Tinnefeld P., Sauer M. (2008) **Subdiffraction-resolution fluorescence imaging with conventional fluorescent probes** *Angew Chem Int Ed Engl* **47**:6172–6176

30. Hirumi H., Hirumi K. (1989) **Continuous cultivation of Trypanosoma brucei blood stream forms in a medium containing a low concentration of serum protein without feeder cell layers** *J Parasitol* **75**:985–989

31. Jones N.G., Thomas E.B., Brown E., Dickens N.J., Hammarton T.C., Mottram J.C. (2014) **Regulators of Trypanosoma brucei cell cycle progression and differentiation identified using a kinome-wide RNAi screen** *PLoS Pathog* **10**

32. Kalichava A., Ochsenreiter T. (2021) **Ultrastructure expansion microscopy in Trypanosoma brucei** *Open Biology* **11**

33. Link F., Borges A.R., Jones N.G., Engstler M. (2021) **To the Surface and Back: Exo- and Endocytic Pathways in Trypanosoma brucei** *Front Cell Dev Biol* **9**

34. Mayor S., Presley J.F., Maxfield F.R. (1993) **Sorting of membrane components from endosomes and subsequent recycling to the cell surface occurs by a bulk flow process** *Journal of Cell Biology* **121**:1257–1269

35. McGovern O.L., Rivera-Cuevas Y., Carruthers V.B. (2021) **Emerging Mechanisms of Endocytosis in Toxoplasma gondii** *Life* **11**

36. Minamino N., Ueda T. (2019) **RAB GTPases and their effectors in plant endosomal transport** *Current Opinion in Plant Biology* **52**:61–68

37. Möbius W., Posthuma G. (2019) **Sugar and ice: Immunoelectron microscopy using cryosections according to the Tokuyasu method** *Tissue Cell* **57**:90–102

38. Morgan G.W., Allen C.L., Jeffries T.R., Hollinshead M., Field M.C. (2001) **Developmental and morphological regulation of clathrin-mediated endocytosis in Trypanosoma brucei** *J Cell Sci* **114**:2605–2615

39. Mugnier M.R., Stebbins C.E., Papavasiliou F.N. (2016) **Masters of Disguise: Antigenic Variation and the VSG Coat in Trypanosoma brucei** *PLoS Pathog* **12**

40. Overath P., Engstler M. (2004) **Endocytosis, membrane recycling and sorting of GPI-anchored proteins: Trypanosoma brucei as a model system** *Mol Microbiol* **53**:735–744

41. Overath P., Stierhof Y.D., Wiese M. (1997) **Endocytosis and secretion in trypanosomatid parasites - Tumultuous traffic in a pocket** *Trends Cell Biol* **7**:27–33

42. Pal A., Hall B.S., Jeffries T.R., Field M.C. (2003) **Rab5 and Rab11 mediate transferrin and anti-variant surface glycoprotein antibody recycling in Trypanosoma brucei** *Biochem J* **374**:443–451

43. Podinovskaia M., Prescianotto-Baschong C., Buser D.P., Spang A. (2021) **A novel live-cell imaging assay reveals regulation of endosome maturation** *Elife* **10**

44. Podinovskaia M., Spang A., Lamaze C., Prior I. (2018) **The Endosomal Network: Mediators and Regulators of Endosome Maturation** *Endocytosis and Signaling* :1–38

45. Porto-Carreiro I., Attias M., Miranda K., De Souza W., Cunha-e-Silva N. (2000) **Trypanosoma cruzi epimastigote endocytic pathway: cargo enters the cytostome and passes through an early endosomal network before storage in reservosomes** *Eur J Cell Biol* **79**:858–869

46. Poteryaev D., Datta S., Ackema K., Zerial M., Spang A. (2010) **Identification of the switch in early-to-late endosome transition** *Cell* **141**:497–508

47. Redmond S., Vadivelu J., Field M.C. (2003) **RNAit: an automated web-based tool for the selection of RNAi targets in Trypanosoma brucei** *Mol Biochem Parasitol* **128**:115–118

48. Rink J., Ghigo E., Kalaidzidis Y., Zerial M. (2005) **Rab conversion as a mechanism of progression from early to late endosomes** *Cell* **122**:735–749

49. Rose C. *et al.* (2020) **Trypanosoma brucei colonizes the tsetse gut via an immature peritrophic matrix in the proventriculus** *Nature Microbiology* **5**:909–916

50. Schwebs M., Paul T., Glogger M., Forster L., Morriswood B., Teßmar J., Groll J., Engstler M., Kollmannsberger P., Fenz S. (2022) **Single-molecule fluorescence microscopy demonstrates fast dynamics of the variant surface glycoprotein coat on living trypanosomes** *bioRxiv*

51. Silverman J.S., Schwartz K.J., Hajduk S.L., Bangs J.D. (2011) **Late endosomal Rab7 regulates lysosomal trafficking of endocytic but not biosynthetic cargo in Trypanosoma brucei** *Mol Microbiol* **82**:664–678

52. Slot J.W., Geuze H.J. (2007) **Cryosectioning and immunolabeling** *Nat Protoc* **2**:2480–2491

53. Stoorvogel W., Strous G.J., Geuze H.J., Oorschot V., Schwartz A.L. (1991) **Late endosomes derive from early endosomes by maturation** *Cell* **65**:417–427

54. Strassert J.F.H., Irisarri I., Williams T.A., Burki F. (2021) **A molecular timescale for eukaryote evolution with implications for the origin of red algal-derived plastids** *Nat Commun* **12**

55. Taylor J.E., Rudenko G. (2006) **Switching trypanosome coats: what's in the wardrobe?** *Trends in Genetics* **22**:614–620

56. Tazeh N.N., Silverman J.S., Schwartz K.J., Sevova E.S., Sutterwala S.S., Bangs J.D. (2009) **Role of AP-1 in developmentally regulated lysosomal trafficking in Trypanosoma brucei** *Eukaryot Cell* **8**:1352–1361

57. Tillberg P.W. *et al.* (2016) **Protein-retention expansion microscopy of cells and tissues labeled using standard fluorescent proteins and antibodies** *Nat Biotechnol* **34**:987–992

58. Triggs V.P., Bangs J.D. (2003) **Glycosylphosphatidylinositol-dependent protein trafficking in bloodstream stage Trypanosoma brucei** *Eukaryot Cell* **2**:76–83

59. van der Beek J., de Heus C., Liv N., Klumperman J. (2021) **Quantitative correlative microscopy reveals the ultrastructural distribution of endogenous endosomal proteins** *Journal of Cell Biology* **221**

60. Vines J.H., King J.S. (2019) **The endocytic pathways of Dictyostelium discoideum** *Int J Dev Biol* **63**:461–471

61. Wirtz E., Leal S., Ochatt C., Cross G.A. (1999) **A tightly regulated inducible expression system for conditional gene knock-outs and dominant-negative genetics in Trypanosoma brucei** *Mol Biochem Parasitol* **99**:89–101

Article and author information

Fabian Link
Department of Cell & Developmental Biology, Biocentre, University of Würzburg, 97074 Würzburg, Germany
ORCID iD: 0000-0002-9828-2012

Alyssa Borges
Department of Cell & Developmental Biology, Biocentre, University of Würzburg, 97074 Würzburg, Germany
ORCID iD: 0000-0002-2359-1371

Oliver Karo
Department of Cell & Developmental Biology, Biocentre, University of Würzburg, 97074 Würzburg, Germany

Marvin Jungblut
Department of Biotechnology & Biophysics, Biocentre, University of Würzburg, 97074 Würzburg, Germany
ORCID iD: 0009-0003-2950-6961

Thomas Müller
Department of Cell & Developmental Biology, Biocentre, University of Würzburg, 97074 Würzburg, Germany

Elisabeth Meyer-Natus
Department of Cell & Developmental Biology, Biocentre, University of Würzburg, 97074 Würzburg, Germany

Timothy Krüger
Department of Cell & Developmental Biology, Biocentre, University of Würzburg, 97074 Würzburg, Germany

Stefan Sachs
Department of Biotechnology & Biophysics, Biocentre, University of Würzburg, 97074 Würzburg, Germany

Nicola G. Jones
Department of Cell & Developmental Biology, Biocentre, University of Würzburg, 97074 Würzburg, Germany
ORCID iD: 0000-0003-3384-0156

Mary Morphew
Molecular, Cellular & Developmental Biology, University of Boulder, Colorado, USA
ORCID iD: 0000-0001-5852-6839

Markus Sauer
Department of Biotechnology & Biophysics, Biocentre, University of Würzburg, 97074 Würzburg, Germany
ORCID iD: 0000-0002-1692-3219

Christian Stigloher
Imaging Core Facility, Biocentre, University of Würzburg, 97074 Würzburg, Germany
ORCID iD: 0000-0001-6941-2669

J. Richard McIntosh
Molecular, Cellular & Developmental Biology, University of Boulder, Colorado, USA

Markus Engstler
Department of Cell & Developmental Biology, Biocentre, University of Würzburg, 97074 Würzburg, Germany
For correspondence: markus.engstler@uni-wuerzburg.de
ORCID iD: 0000-0003-1436-5759

Copyright

Editors

Reviewing Editor
Dominique Soldati-Favre
University of Geneva, Geneva, Switzerland

Senior Editor
Dominique Soldati-Favre
University of Geneva, Geneva, Switzerland

Reviewer #2 (Public Review):

The authors suggest that the African trypanosome endomembrane system has unusual organisation, in that the entire system is a single reticulated structure. It is not clear if this is thought to extend to the lysosome or MVB. There is also a suggestion that this unusual morphology serves as a trans-(post)Golgi network rather than the more canonical arrangement.

The updated manuscript is significantly improved. I remain at slight odds with the author's push for the lack of generality as important, and the new cell biology that we have been on the verge of for decades. However, that is a scholarly issue and is not grounds for any further revision of the present manuscript.

https://doi.org/10.7554/eLife.91194.2.sa1

Reviewer #3 (Public Review):

Summary:
A key element in the ability of trypanosomes to evade the mammalian host's immune system is its high rate of endocytosis. This rapid turnover of its surface enables the trypanosome to 'clean' its surface removing antibodies and other immune effectors that are subsequently degraded. The high rate of endocytosis is likely reflected in the organisation of the endosomal system in these parasites. Here, Link et al., sought to address this question using a range of light and three-dimensional electron microscopy approaches to define the endosomal organisation in this parasite.

Before this study, the vast majority of our information about the make-up of the trypanosome endosomal system was from thin section electron microscopy and immunofluorescence studies, which did not provide the necessary resolution and 3D information to address this issue. Therefore, it was not known how the different structures observed by EM were related. Link et al., have taken advantage of the advances in technology and used an impressive combination of approaches at the LM and EM level to study the endosomal system in these parasites. This innovative combination has now shown the interconnected-ness of this network and demonstrated that there are no 'classical' compartments within the endosomal system, with instead different regions of the network enriched in different protein markers (Rab5a, Rab7, Rab11). Overall, the authors have achieved their aims, with results supporting their conclusions.

This is a well written manuscript in which the authors use an impressive range of approaches to address the organisation of the endosomal system. The authors have clearly demonstrated that trypanosomes have a large interconnected endosomal network, without defined compartments and instead shows enrichment for specific Rabs within this network. I appreciate their inclusion of how they used a range of different light microscopy approaches even though for instance the dSTORM approach did not turn out to be as effective as hoped.

The methodological impact of this work has the potential to be large, as the authors have introduced a range of advanced EM techniques for the study of trypanosomes. Moreover, the study of fundamental biological processes such as endosomal trafficking in divergent eukaryotes is important to define the limits within which this process operates.

https://doi.org/10.7554/eLife.91194.2.sa0

Author Response

The following is the authors' response to the original reviews.

> ***eLife assessment***
>
> *This important study combines a range of advanced ultrastructural imaging approaches to define the unusual endosomal system of African trypanosomes. Compelling images show that instead of a distinct set of compartments, the endosome of these protists comprises a continuous system of membranes with functionally distinct subdomains as defined by canonical markers of early, late and recycling endosomes. The findings suggest that the endocytic system of bloodstream stages has evolved to facilitate the extraordinarily high rates of membrane turnover needed to remove immune complexes and survive in the blood, which is of interest to anyone studying infectious diseases.*
>
> ***Public Reviews:***
>
> ***Reviewer #1 (Public Review):***

Summary:

Bloodstream stages of the parasitic protist, Trypanosoma brucei, exhibit very high rates of constitutive endocytosis, which is needed to recycle the surface coat of Variant Surface Glycoproteins (VSGs) and remove surface immune complexes. While many studies have shown that the endo-lysosomal systems of T. brucei BF stages contain canonical domains, as defined by classical Rab markers, it has remained unclear whether these protists have evolved additional adaptations/mechanisms for sustaining these very high rates of membrane transport and protein sorting. The authors have addressed this question by reconstructing the 3D ultrastructure and functional domains of the T. brucei BF endosome membrane system using advanced electron tomography and super-resolution microscopy approaches. Their studies reveal that, unusually, the BF endosome network comprises a continuous system of cisternae and tubules that contain overlapping functional subdomains. It is proposed that a continuous membrane system allows higher rates of protein cargo segregation, sorting and recycling than can otherwise occur when transport between compartments is mediated by membrane vesicles or other fusion events.

Strengths:

The study is a technical tour-de-force using a combination of electron tomography, super-resolution/expansion microscopy, immune-EM of cryo-sections to define the 3D structures and connectivity of different endocytic compartments. The images are very clear and generally support the central conclusion that functionally distinct endocytic domains occur within a dynamic and continuous endosome network in BF stages.

Weaknesses:

The authors suggest that this dynamic endocytic network may also fulfil many of the functions of the Golgi TGN and that the latter may be absent in these stages. Although plausible, this comment needs further experimental support. For example, have the authors attempted to localize canonical makers of the TGN (e.g. GRIP proteins) in T. brucei BF and/or shown that exocytic carriers bud directly from the endosomes?

We agree with the criticism and have shortened the discussion accordingly and clearly marked it as speculation. However, we do not want to completely abandon our hypothesis.

The paragraph now reads:

Lines 740 – 751:

“Interestingly, we did not find any structural evidence of vesicular retrograde transport to the Golgi. Instead, the endosomal ‘highways’ extended throughout the posterior volume of the trypanosomes approaching the trans-Golgi interface. It is highly plausible that this region represents the convergence point where endocytic and biosynthetic membrane trafficking pathways merge. A comparable merging of endocytic and biosynthetic functions has been described for the TGN in plants. Different marker proteins for early and recycling endosomes were shown to be associated and/ or partially colocalized with the TGN suggesting its function in both secretory and endocytic pathways (reviewed in Minamino and Ueda, 2019). As we could not find structural evidence for the existence of a TGN we tentatively propose that trypanosomes may have shifted the central orchestrating function of the TGN as a sorting hub at the crossroads of biosynthetic and recycling pathways to the endosome. Although this is a speculative scenario, it is experimentally testable.”

Furthermore, we removed the lines 51 - 52, which included the suggestion of the TGN as a master regulator, from the abstract.

> ***Reviewer #2 (Public Review):***
>
> *The authors suggest that the African trypanosome endomembrane system has unusual organisation, in that the entire system is a single reticulated structure. It is not clear if this is thought to extend to the lysosome or MVB. There is also a suggestion that this unusual morphology serves as a trans-(post)Golgi network rather than the more canonical arrangement.*
>
> *The work is based around very high-quality light and electron microscopy, as well as utilising several marker proteins, Rab5A, 11 and 7. These are deemed as markers for early endosomes, recycling endosomes and late or pre-lysosomes. The images are mostly of high quality but some inconsistencies in the interpretation, appearance of structures and some rather sweeping assumptions make this less easy to accept. Two perhaps major issues are claims to label the entire endosomal apparatus with a single marker protein, which is hard to accept as certainly this reviewer does not really even know where the limits to the endosomal network reside and where these interface with other structures. There are several additional compartments that have been defined by Rob proteins as well, and which are not even mentioned. Overall I am unconvinced that the authors have demonstrated the main things they claim.*
> *The endomembrane system in bloodstream form T. brucei is clearly delimited. Compared to mammalian cells it is tidy and confined to the posterior part of the spindleshaped cell. The endoplasmic reticulum is linked to one side of the longitudinal cell axis, marked by the attached flagellum, while the mitochondrion locates to the opposite side. Glycosomes are easily identifiable as spheres, as are acidocalcisomes, which are smaller than glycosomes and – in electron micrographs – are characterized by high electron density. All these organelles extend beyond the nucleus, which is not the case for the endosomal compartment, the lysosome and the Golgi. The vesicles found in the posterior half of the trypanosome cell are quantitatively identifiable as COP1, CCVI or CCVII vesicles, or exocytic carriers. The lysosome has a higher degree of morphological plasticity, but this is not topic of the present work. Thus, the endomembrane system in T. brucei is comparatively well structured and delimited, which is why we have chosen trypanosomes as cell biological model.*

We have published EP1::GFP as marker for the endosome system and flagellar pocket back in 2004. We have defined the fluid phase volume of the trypanosome endosome in papers published between 2002 and 2007. This work was not intended to represent the entirety of RAB proteins. We were only interested in 3 canonical markers for endosome subtypes. We do not claim anything that is not experimentally tested, we have clearly labelled our hypotheses as such, and we do not make sweeping assumptions.

> *The approaches taken are state-of-the-art but not novel, and because of the difficulty in fully addressing the central tenet, I am not sure how much of an impact this will have beyond the trypanosome field. For certain this is limited to workers in the direct area and is not a generalisable finding.*

To the best of our knowledge, there is no published research that has employed 3D Tokuyasu or expansion microscopy (ExM) to label endosomes. The key takeaway from our study, which is the concept that "endosomes are continuous in trypanosomes" certainly is novel. We are not aware of any other report that has demonstrated this aspect.

The doubts formulated by the reviewer regarding the impact of our work beyond the field of trypanosomes are not timely. Indeed, our results, and those of others, show that the conclusions drawn from work with just a few model organisms is not generalisable. We are finally on the verge of a new cell biology that considers the plethora of evolutionary solutions

beyond ophistokonts. We believe that this message should be widely acknowledged and considered. And we are certainly not the only ones who are convinced that the term "general relevance" is unscientific and should no longer be used in biology.

> ***Reviewer #3 (Public Review):***
>
> *Summary:*
>
> *As clearly highlighted by the authors, a key plank in the ability of trypanosomes to evade the mammalian host's immune system is its high rate of endocytosis. This rapid turnover of its surface enables the trypanosome to 'clean' its surface removing antibodies and other immune effectors that are subsequently degraded. The high rate of endocytosis is likely reflected in the organisati'n and layout of the endosomal system in these parasites. Here, Link et al., sought to address this question using a range of light and three-dimensional electron microscopy approaches to define the endosomal organisation in this parasite.*
>
> *Before this study, the vast majority of our information about the make-up of the trypanosome endosomal system was from thin-section electron microscopy and immunofluorescence studies, which did not provide the necessary resolution and 3D information to address this issue. Therefore, it was not known how the different structures observed by EM were related. Link et al., have taken advantage of the advances in technology and used an impressive combination of approaches at the LM and EM level to study the endosomal system in these parasites. This innovative combination has now shown the interconnected-ness of this network and demonstrated that there are no 'classical' compartments within the endosomal system, with instead different regions of the network enriched in different protein markers (Rab5a, Rab7, Rab11).*
>
> *Strengths:*
>
> *This is a generally well-written and clear manuscript, with the data well-presented supporting the majority of the conclusions of the authors. The authors use an impressive range of approaches to address the organisation of the endosomal system and the development of these methods for use in trypanosomes will be of use to the wider parasitology community.*
>
> *I appreciate their inclusion of how they used a range of different light microscopy approaches even though for instance the dSTORM approach did not turn out to be as effective as hoped. The authors have clearly demonstrated that trypanosomes have a large interconnected endosomal network, without defined compartments and instead show enrichment for specific Rabs within this network.*
>
> *Weaknesses:*
>
> *My concerns are:*
>
> *i) There is no evidence for functional compartmentalisation. The classical markers of different endosomal compartments do not fully overlap but there is no evidence to show a region enriched in one or other of these proteins has that specific function. The authors should temper their conclusions about this point.*

The reviewer is right in stating that Rab-presence does not necessarily mean Rabfunction. However, this assumption is as old as the Rab literature. That is why we have focused on the 3 most prominent endosomal marker proteins. We report that for endosome function you do not necessarily need separate membrane compartments. This is backed by our experiments.

> *ii) The quality of the electron microscopy work is very high but there is a general lack of numbers. For example, how many tomograms were examined? How often were fenestrated sheets seen? Can the authors provide more information about how frequent these observations were?*

The fenestrated sheets can be seen in the majority of the 37 tomograms recorded of the posterior volume of the parasites. Furthermore, we have randomly generated several hundred tiled (= very large) electron micrographs of bloodstream form trypanosomes for unbiased analyses of endomembranes. In these 2D-datasets the "footprint" of the fenestrated flat and circular cisternae is frequently detectable in the posterior cell area.

We now have included the corresponding numbers in all EM figure legends.

> *iii) The EM work always focussed on cells which had been processed before fixing. Now, I understand this was important to enable tracers to be used. However, given the dynamic nature of the system these processing steps and feeding experiments may have affected the endosomal organisation. Given their knowledge of the system now, the authors should fix some cells directly in culture to observe whether the organisation of the endosome aligns with their conclusions here.*

This is a valid criticism; however, it is the cell culture that provides an artificial environment. As for a possible effect of cell harvesting by centrifugation on the integrity and functionality of the endosome system, we consider this very unlikely for one simple reason. The mechanical forces acting in and on the parasites as they circulate in the extremely crowded and confined environment of the mammalian bloodstream are obviously much higher than the centrifugal forces involved in cell preparation. This becomes particularly clear when one considers that the mass of the particle to be centrifuged determines the actual force exerted by the g-forces. Nevertheless, the proposed experiment is a good control, although much more complex than proposed, since tomography is a challenging technique. We have performed the suggested experiment and acquired tomograms of unprocessed cells. The corresponding data is now included as supplementary movie 2, 3 and 4. We refer to it in lines 202 – 206: To investigate potential impacts of processing steps (cargo uptake, centrifugation, washing) on endosomal organization, we directly fixed cells in the cell culture flask, embedded them in Epon, and conducted tomography. The resulting tomograms revealed endosomal organization consistent with that observed in cells fixed after processing (see Supplementary movie 2, 3, and 4).

We furthermore thank the reviewer for the experiment suggestion in the acknowledgments.

> *iv) The discussion needs to be revamped. At the moment it is just another run through of the results and does not take an overview of the results presenting an integrated view. Moreover, it contains reference to data that was not presented in the results.*

We have improved the discussion accordingly.

> ***Recommendations for the authors:***
>
> *The reviewers concurred about the high calibre of the work and the importance of the findings.*
>
> *They raised some issues and made some suggestions to improve the paper without additional experiments - key issues include*
>
> *(1) Better referencing of the trypanosome endocytosis/ lysosomal trafficking literature.*

The literature, especially the experimental and quantitative work, is very limited. We now provide a more complete set of references. However, we would like to mention that we had cited a recent review that critically references the trypanosome literature with emphasis on the extensive work done with mammalian cells and yeast.

> *(2) Moving the dSTORM data that detracts from otherwise strong data in a supplementary figure.*

We have done this.

> *(3) Removal of the conclusion that the continuous endosome fulfils the functions of TGN, without further evidence.*

As stated above, this was not a conclusion in our paper, but rather a speculation, which we have now more clearly marked as such. Lines 740 to 751 now read:

"Interestingly, we did not find any structural evidence of vesicular retrograde transport to the Golgi. Instead, the endosomal 'highways' extended throughout the posterior volume of the trypanosomes approaching the trans-Golgi interface. It is highly plausible that this region represents the convergence point where endocytic and biosynthetic membrane trafficking pathways merge. A comparable merging of endocytic and biosynthetic functions was already described for the TGN in plants. Different marker proteins for early and recycling endosomes were shown to be associated and/ or partially colocalized with the TGN suggesting its function in both secretory and endocytic pathways (reviewed in Minamino and Ueda, 2019). As we could not find structural evidence for the existence of a TGN we tentatively propose that trypanosomes may have shifted the central orchestrating function of the TGN as a sorting hub at the crossroads of biosynthetic and recycling pathways to the endosome. Although this is a speculative scenario, it is experimentally testable."

> *(4) Broader discussion linking their findings to other examples of organelle maturation in eukaryotes (e.g cisternal maturation of the Golgi)*

We have improved the discussion accordingly.

> ***Reviewer #1 (Recommendations For The Authors):***
>
> *What are the multi-vesicular vesicles that surround the marked endosomal compartments in Fig 1. Do they become labelled with fluid phase markers with longer incubations (e.g late endosome/ lysosomal)?*

The function of MVBs in trypanosomes is still far from being clear. They are filled with fluid phase cargo, especially ferritin, but are devoid of VSG. Hence it is likely that MVBs are part of the lysosomal compartment. In fact, this part of the endomembrane system is highly dynamic. MVBs can be physically connected to the lysosome or can form elongated structures. The surprising dynamics of the trypanosome lysosome will be published elsewhere.

> *Figure 2. The compartments labelled with EP1::Halo are very poorly defined due to the low levels of expression of the reporter protein and/or sensitivity of detection of the Halo tag. Based on these images, it would be hard to conclude whether the endosome network is continuous or not. In this respect, it is unclear why the authors didn't use EP1-GFP for these analyses? Given the other data that provides more compelling evidence for a single continuous compartment, I would suggest removing Fig 2A.*

We have used EP1::GFP to label the entire endosome system (Engstler and Boshart, 2004). Unfortunately, GFP is not suited for dSTORM imaging. By creating the EP1::Halo cell line, we were able to utilize the most prominent dSTORM fluorescent dye, Alexa 647. This was not primarily done to generate super resolution images, but rather to measure the dynamics of the GPI-anchored, luminal protein EP with single molecule precision. The results from this study will be published separately. But we agree with the reviewer and have relocated the dSTORM data to the supplementary material.

> *The observation that Rab5a/7 can be detected in the lumen of lysosome is interesting. Mechanistically, this presumably occurs by invagination of the limiting membrane of the lysosome. Is there any evidence that similar invagination of cytoplasmic markers occurs throughout or in subdomains of the endocytic network (possibly indicative of a 'late endosome' domain)?*

So far, we have not observed this. The structure of the lysosome and the membrane influx from the endosome are currently being investigated.

> *The authors note that continuity of functionally distinct membrane compartments in the secretory/endocytic pathways has been reported in other protists (e.g T. cruzi). A particular example that could be noted is the endo-lysosomal system of Dictyostelium discoideum which mediates the continuous degradation and eventual expulsion of undigested material.*

We tried to include this in the discussion but ultimately decided against it because the Dictyostelium system cannot be easily compared to the trypanosome endosome.

> ***Reviewer #2 (Recommendations For The Authors):***
>
> *Abstract*
>
> *Not sure that 'common' is the correct term here. Frequent, near-universal..... it would be true that endocytosis is common across most eukaryotes.*

We have changed the sentence to “common process observed in most eukaryotes” (line 33).

> *Immune evasion - the parasite does not escape the immune system, but does successfully avoid its impact, at least at the population level.*

We have replaced the word “escape” with “evasion” (line 35).

> *The third sentence needs to follow on correctly from the second. Also, more than Igs are internalised and potentially part of immune evasion, such as C3, Factor H, ApoL1 etcetera.*

We believe that there may be a misunderstanding here. The process of endocytic uptake and lysosomal degradation has so far only been demonstrated in the context of VSGbound antibodies, which is why we only refer to this. Of course, the immune system comprises a wide range of proteins and effector molecules, all of which could be involved in immune evasion.

> *I do not follow the logic that the high flux through the endocytic system in trypanosomes precludes distinct compartmentalisation - one could imagine a system where a lot of steps become optimised for example. This idea needs expanding on if it is correct.*

Membrane transport by vesicle transfer between several separate membrane compartments would be slower than the measured rate of membrane flux.

> *Again I am not sure 'efficient' on line 40. It is fast, but how do you measure efficiency? Speed and efficiency are not the same thing.*

We have replaced the word “efficient” with “fast” (line 42).

> *The basis for suggesting endosomes as a TGN is unclear. Given that there are AP complexes, retromer, exocyst and other factors that are part of the TGN or at least post-G differentiation of pathways in canonical systems, this seems a step too far. There really is no evidence in the rest of the MS that seems to support this.*

Yes, we agree and have clarified the discussion accordingly. We have not completely removed the discussion on the TGN but have labelled it more clearly as speculation.

> *I am aware I am being pedantic here, but overall the abstract seems to provide an impression of greater novelty than may be the case and makes several very bold claims that I cannot see as fully valid.*

We are not aware of any claim in the summary that we have not substantiated with experiments, or any hypothesis that we have not explained.

> *Moreover, the concept of fused or multifunctional endosomes (or even other endomembrane compartments) is old, and has been demonstrated in metazoan cells and yeast. The concept of rigid (in terms of composition) compartments really has been rejected by most folks with maturation, recycling and domain structures already well-established models and concepts.*

We agree that the (transient) presence of multiple Rab proteins decorating endosomes has been demonstrated in various cell types. This finding formed the basis for the endosomal maturation model in mammals and yeast, which has replaced the previous rigid compartment model.

However, we do not appreciate attempts to question the originality of our study by claiming that similar observations have been made in metazoans or yeast. This is simply wrong. There are no reports of a functionally structured, continuous, single and large endosome in any other system. The only membrane system that might be similar was described in the American parasite Trypanosoma cruzi, however, without the use of endosome markers or any functional analysis. We refer to this study in the discussion.

In summary, the maturation model falls short in explaining the intricacies of the membrane system we have uncovered in trypanosomes. Therefore, one plausible interpretation of our data is that the overall architecture of the trypanosome endosomes represents an adaptation that enables the remarkable speed of plasma membrane recycling observed in these parasites. In our view, both our findings and their interpretation are novel and worth reporting. Again, modern cell biology should recognize that evolution has developed many solutions for similar processes in cells, about whose diversity we have learned almost nothing because of our reductionist view. A remarkable example of this are the Picozoa, tiny bipartite eukaryotes that pack the entire nutritional apparatus into one pouch and the main organelles with the locomotor system into the other. Another one is the “extreme” cell biology of many protozoan parasites such as Giardia, Toxpoplasma or Trypanosoma.

> *Higher plants have been well characterised, especially at the level of Rab/Arf proteins and adaptins.*

We now mention plant endosomes in our brief discussion of the trypanosome TGN. Lines 744 – 747:

“A comparable merging of endocytic and biosynthetic functions was already described for the TGN in plants. Different marker proteins for early and recycling endosomes were shown to be associated and/ or partially colocalized with the TGN suggesting its function in both secretory and endocytic pathways (reviewed in Minamino and Ueda, 2019).”

> *The level of self-citing in the introduction is irritating and unscholarly. I have no qualms with crediting the authors with their own excellent contributions, but work from Dacks, Bangs, Field and others seems to be selectively ignored, with an awkward use of the authors' own publications. Diversity between organisms for example has been a mainstay of the Dacks lab output, Rab proteins and others from Field and work on exocytosis and late endosomal systems from Bangs. These efforts and contributions surely deserve some recognition?*

This is an original article and not a review. For a comprehensive overview the reviewer might read our recent overview article on exo- and endocytic pathways in trypanosomes, in which we have extensively cited the work of Mark Field, Jay Bangs and Joel Dacks. In the present manuscript, we have cited all papers that touch on our results or are otherwise important for a thorough understanding of our hypotheses. We do not believe that this approach is unscientific, but rather improves the readability of the manuscript. Nevertheless, we have now cited additional work.

> *For the uninitiated, the posterior/anterior axis of the trypanosome cell as well as any other specific features should be defined.*

In lines 102 - 110 we wrote:

“This process of antibody clearance is driven by hydrodynamic drag forces resulting from the continuous directional movement of trypanosomes (Engstler et al., 2007). The VSG-antibody complexes on the cell surface are dragged against the swimming direction of the parasite and accumulate at the posterior pole of the cell. This region harbours an invagination in the plasma membrane known as the flagellar pocket (FP) (Gull, 2003; Overath et al., 1997). The FP, which marks the origin of the single attached flagellum, is the exclusive site for endo- and exocytosis in trypanosomes (Gull, 2003; Overath et al., 1997). Consequently, the accumulation of VSG-antibody complexes occurs precisely in the area of bulk membrane uptake.”

We think this sufficiently introduces the cell body axes.

> *I don't understand the comment concerning microtubule association. In mammalian cells, such association is well established, but compartments still do not display precise positioning. This likely then has nothing to do with the microtubule association differences.*

We have clarified this in the text (lines 192 – 199). There is no report of cytoplasmic microtubules in trypanosomes. All microtubules appear to be either subpellicular or within the flagellum. To maintain the structure and position of the endosomal apparatus, they should be associated either with subpellicular microtubules, as is the case with the endoplasmic reticulum, or with the more enigmatic actomyosin system of the parasites. We

have been working on the latter possibility and intend to publish a follow-up paper to the present manuscript.

> *The inability to move past the nucleus is a poor explanation. These compartments are dynamic. Even the nucleus does interesting things in trypanosomes and squeezes past structures during development in the tsetse fly.*

The distance between the nucleus and the microtubule cytoskeleton remains relatively constant even in parasites that squeeze through microfluidic channels. This is not unexpected as the nucleus can be highly deformed. A structure the size of the endosome will not be able to physically pass behind the nucleus without losing its integrity. In fact, the recycling apparatus is never found in the anterior part of the trypanosome, most probably because the flagellar pocket is located at the posterior cell pole.

> *L253 What is the evidence that EP1 labels the entire FP and endosomes? This may be extensive, but this claim requires rather more evidence. This is again suggested at l263. Again, please forgive me for being pedantic, but this is an overstatement unless supported by evidence that would be incredibly difficult to obtain. This is even sort of acknowledged on l271 in the context of non-uniform labelling. This comes again in l336.*

The evidence that EP1 labels the entire FP and endosomes is presented here: Engstler and Boshart, 2004; 10.1101/gad.323404).

> *Perhaps I should refrain from comments on the dangers of expansion microscopy, or asking what has actually been gained here. Oddly, the conclusion on l290 is a fair statement that I am happy with.*

An in-depth discussion regarding the advantages and disadvantages of expansion microscopy is beyond the manuscript's intended scope. Our approach involved utilizing various imaging techniques to confirm the validity of our findings. We appreciate that our concluding sentence is pleasing.

> *F2 - The data in panel A seem quite poor to me. I also do not really understand why the DAPI stain in the first and second columns fails to coincide or why the kinetoplast is so diffuse in the second row. The labelling for EP1 presents as very small puncta, and hence is not evidence for a continuum. What is the arrow in A IV top? The data in panel B are certainly more in line with prior art, albeit that there is considerable heterogeneity in the labelling and of the FP for example. Again, I cannot really see this as evidence for continuity. There are gaps.... Albeit I accept that labelling of such structures is unlikely to ever be homogenous.*

We agree that the dSTORM data represents the least robust aspect of the findings we have presented, and we concur with relocating it to the supplementary material.

> *F3 - Rather apparent, and specifically for Rab7, that there is differential representation - for example, Cell 4 presents a single Rab7 structure while the remaining examples demonstrate more extensive labelling. Again, I am content that these are highly dynamic strictures but this needs to be addressed at some level and commented upon. If the claim is for continuity, the dynamics observed here suggest the usual; some level of obvious overlap of organellar markers, but the representation in F3 is clever but not sure what I am looking at. Moreover, the title of the figure is nothing new. What is also a bit odd is that the extent of the Rab7 signal, and to some extent the other two Rabs used, is rather variable, which makes this unclear to me as to what is being detected. Given that the Rab*

> *proteins may be defining microdomains or regions, I would also expect a region of unique straining as well as the common areas. This needs to at least be discussed.*

The differences in the representation result from the dynamics of the labelled structures. Therefore, we have selected different cells to provide examples of what the labelling can look like. We now mention this in the results section.

The overlap of the different Rab signals was perhaps to be expected, but we now have demonstrated it experimentally. Importantly, we performed a rigorous quantification by calculating the volume overlaps and the Pearson correlation coefficients.

In previous studies the data were presented as maximal intensity projections, which inherently lack the complete 3D information.

We found that Rab proteins define microdomains and that there are regions of unique staining as well as common areas, as shown in Figure 3. The volumes do not completely overlap. This is now more clearly stated in lines 315 – 319:

“These objects showed areas of unique staining as well as partially overlapping regions. The pairwise colocalization of different endosomal markers is shown in Figure 3 A, XI - XIII and 3 B. The different cells in Figure 3 B were selected to represent the dynamic nature of the labelled structures. Consequently, the selected cells provide a variety of examples of how the labelling can appear.”

This had already been stated in lines 331 – 336:

“In summary, the quantitative colocalization analyses revealed that on the one hand, the endosomal system features a high degree of connectivity, with considerable overlap of endosomal marker regions, and on the other hand, TbRab5A, TbRab7, and TbRab11 also demarcate separated regions in that system. These results can be interpreted as evidence of a continuous endosomal membrane system harbouring functional subdomains, with a limited amount of potentially separated early, late or recycling endosomes.”

> *F4-6 - Fabulous images. But a couple of issues here; first, as the authors point out, there is distance between the gold and the antigen. So, this of course also works in the z-plane as well as the x/y-planes and some of the gold may well be associated with membraneous figures that are out of the plane, which would indicate an absence of colinearity on one specific membrane. Secondly, in several instances, we have Rab7 essentially mixed with Rab11 or Rab5 positive membrane. While data are data and should be accepted, this is difficult to reconcile when, at least to some level, Rab7 is a marker for a late-endosomal structure and where the presence of degradative activity could reside. As division of function is, I assume, the major reason for intracellular compartmentalisation, such a level of admixture is hard to rationalise. A continuum is one thing but the data here seem to be suggesting something else, i.e. almost complete admixture.*

We are grateful for the positive feedback regarding the image quality. It is true that the "linkage error," representing the distance between the gold and the antigen, also functions to some extent in the z-axis. However, it's important to note that the zdimension of the section in these Figures is 55 nm. Nevertheless, it's interesting to observe that membranes, which may not be visible within the section itself but likely the corresponding Rab antigen, is discernible in Figure 4C (indicated by arrows).

We have clarified this in lines 397 – 400:

“Consequently, gold particles located further away may represent cytoplasmic TbRab proteins or, as the “linkage error” can also occur in the z-plane, correspond to membranes that are not

visible within the 55 nm thickness of the cryosection (Figure 4, panel C, arrows). “

The coexistence of different Rabs is most likely concentrated in regions where transitions between different functions are likely. Our focus was primarily on imaging membranes labelled with two markers. We wanted to show that the prevailing model of separate compartments in the trypanosome literature is not correct.

> *F7 - Not sure what this adds beyond what was published by Grunfelder.*

First, this figure is an important control that links our results to published work (Grünfelder et al. (2003)). Second, we include double staining of cargo with Rab5, Rab7, and Rab11, whereas Grünfelder focused only on Rab11. Therefore, our data is original and of such high quality that it warrants a main figure.

> *F8 - and l583. This is odd as the claim is 'proof' which in science is a hard thing to claim (and this is definitely not at a six sigma level of certainty, as used by the physics community). However, I am seeing structures in the tomograms which are not contiguous - there are gaps here between the individual features (Green in the figure).*

We have replaced the term "proof". It is important to note that the structures in individual tomograms cannot all be completely continuous because the sections are limited to a thickness of 250 nm. Therefore, it is likely that they have more connectivity above and below the imaged section. Nevertheless, we believe that the quality of the tomograms is satisfactory, considering that 3D Tokuyasu is a very demanding technique and the production of serial Tokuyasu tomograms is not feasible in practice.

> *Discussion - Too long and the self-citing of four papers from the corresponding author to the exclusion of much prior work is again noted, with concerns about this as described above. Moreover, at least four additional Rab proteins are known associated with the trypanosome endosomal system, 4, 5B, 21 and 28. These have been completely ignored.*

We have outlined our position on referencing in original articles above. We also explained why we focused on the key marker proteins associated with early (Rab5), late (Rab7) and recycling endosomes (Rab11). We did not ignore the other Rabs, we just did not include them in the present study.

> *Overall this is disappointing. I had expected a more robust analysis, with a clearer discussion and placement in context. I am not fully convinced that what we have here is as extreme as claimed, or that we have a substantial advance. There is nothing here that is mechanistic or the identification of a new set of gene products, process or function.*

We do not think that this is constructive feedback.

> *This MS suggests that the endosomal system of African trypanosomes is a continuum of membrane structures rather than representing a set of distinct compartments. A combination of light and electron microscopy methods are used in support. The basic contention is very challenging to prove, and I'm not convinced that this has been. Furthermore, I am also unclear as to the significance of such an organisation; this seems not really addressed.*

We acknowledge and respect varying viewpoints, but we hold a differing perspective in this matter. We are convinced that the data decisively supports our interpretation. May future work support or refute our hypothesis.

> ***Reviewer #3 (Recommendations For The Authors):***
>
> *Line 81 - delete 's*

Done.

> *Generally, the introduction was very well written and clearly summarised our current understanding but the paragraph beginning line 134 felt out of place and repeated some of the work mentioned earlier.*

We have removed this paragraph.

> *For the EM analysis throughout quantification would be useful as highlighted in the public review. How many tomograms were examined, and how often were types of structures seen? I understand the sample size is often small but this would help the reader appreciate the diversity of structures seen.*

We have included the numbers.

> *Following on from this how were the cells chosen for tomogram analysis? For example, the dividing cell in 1D has palisades associating with the new pocket - is this commonly seen? Does this reflect something happening in dividing cells. This point about endosomal division was picked up in the discussion but there was little about in the main results.*

This issue is undoubtedly inherent to the method itself, and we have made efforts to mitigate it by generating a series of tomograms recorded randomly. We have refrained from delving deeper into the intricacies of the cell cycle in this manuscript, as we believe that it warrants a separate paper.

> *As the authors prosecute, the co-localisation analysis highlights the variable nature of the endosome and the overlap of different markers. When looking at the LM analysis, I was struck by the variability in the size and number of labelled structures in the different cells. For example, in 3A Rab7 is 2 blobs but in 3B Cell 1 it is 4/5 blobs. Is this just a reflection of the increase in the endosome during the cell cycle?*

The variability in representation is a direct consequence of the dynamic nature of the labelled structures. For this reason, we deliberately selected different cells to represent examples of how the labelling can look like. We have decided not to mention the dynamics of the endosome during the cell cycle. This will be the subject of a further report.

> *Moreover, Rab 11 looks to be the marker covering the greatest volume of the endosomal system - is this true? I think there's more analysis of this data that could be done to try and get more information about the relative volumes etc of the different markers that haven't been drawn out. The focus here is on the co-localisation.*

Precisely because we recognize the importance of this point, we intend to turn our attention to the cell cycle in a separate publication.

> *I appreciate that it is an awful lot of work to perform the immuno-EM and the data is of good quality but in the text, there could be a greater effort to tie this to the LM data. For example, from the Rab11 staining in LM you would expect this marker to be the most extensive across the networks - is this reflected in the EM?*

> *For the immuno-EM there were no numbers, the authors had measured the position of the gold but what was the proportion of gold that was in/near membranes for each marker? This would help the reader understand both the number of particles seen and the enrichment of the different regions.*

Our original intent was to perform a thorough quantification (using stereology) of the immuno-EM data. However, we later realized that the necessary random imaging approach is not suitable for Tokuyasu sections of trypanosomes. In short, the cells are too far apart, and the cell sections are only occasionally cut so that the endosomal membranes are sufficiently visible. Nevertheless, we continue to strive to generate more quantitative data using conventional immuno-EM.

> *The innovative combination of Tokuyasu tomograms with immuno-EM was great. I noted though that there was a lack of fenestration in these models. Does this reflect the angle of the model or the processing of these samples?*

We are grateful to the referee, as we have asked ourselves the same question. However, we do not attribute the apparent lack of fenestration to the viewing angle, since we did not find fenestration in any of the Tokuyasu tomograms. Our suspicion is more directed towards a methodological problem. In the Tokuyasu workflow, all structures are mainly fixed with aldehydes. As a result, lipids are only effectively fixed through their association with membrane proteins. We suggest that the fenestration may not be visible because the corresponding lipids may have been lost due to incomplete fixation.

We now clearly state this in the lines 563 – 568.

“Interestingly, these tomograms did not exhibit the fenestration pattern identified in conventional electron tomography. We suspect that this is due to methodological reasons. The Tokuyasu procedure uses only aldehydes to fix all structures. Consequently, effective fixation of lipids occurs only through their association with membrane proteins. Thus, the lack of visible fenestration is likely due to possible loss of lipids during incomplete fixation.”

> *The discussion needs to be reworked. Throughout it contains references to results not in the main results section such as supplementary movie 2 (line 735). The explicit references to the data and figures felt odd and more suited to the results rather than the discussion. Currently, each result is discussed individually in turn and more effort needs to be made to integrate the results from this analysis here but also with previous work and the data from other organisms, which at the moment sits in a standalone section at the end of the discussion.*

We have improved the discussion and removed the previous supplementary movies 2 and 3. Supplementary movie 1 is now mentioned in the results section.

> *Line 693 - There was an interesting point about dividing cells describing the maintenance of endosomes next to the old pocket. Does that mean there was no endosome by the new pocket and if so where is this data in the manuscript? This point relates back to my question about how cells were chosen for analysis - how many dividing cells were examined by tomography?*

The fate of endosomes during the cell cycle is not the subject of this paper. In this manuscript we only show only one dividing cell using tomography. An in-depth analysis focusing on what happens during the cell cycle will be published separately.

> *Line 729 - I'm unclear how this represents a polarization of function in the flagellar pocket. The pocket I presume is included within the endosomal system for this analysis but there was no specific mention of it in the results and no marker of each position to help define any specialisation. From the results, I thought the focus was on endosomal co-localisation of the different markers. If the authors are thinking about specialisation of the pocket this paper from Mark Field shows there is evidence for the exocyst to be distributed over the entire surface of the pocket, which is relevant to the discussion here. Boehm, C.M. et al. (2017) The trypanosome exocyst: a conserved structure revealing a new role in endocytosis. PLoS Pathog. 13, e1006063*

We have formulated our statement more cautiously. However, we are convinced that membrane exchange cannot physically work without functional polarization of the pocket. We know that Rab11, for example, is not evenly distributed on the pocket. By the way, in Boehm et al. (2017) the exocyst is not shown to cover the entire pocket (as shown in Supplementary Video 1).

We now refer to Boehm et al. (Lines 700 – 703):

“Boehm et al (2017) report that in the flagellar pocket endocytic and exocytic sites are in close proximity but do not overlap. We further suggest that the fusion of EXCs with the flagellar pocket membrane and clathrin-mediated endocytosis take place on different sites of the pocket. This disparity explains the lower colocalization between TbRab11 and TbRab5A.”

> *Line 735 - link to data not previously mentioned I think. When I looked at this data I couldn't find a key to explain what all the different colours related to.*

We have removed the previous supplementary movies 2 and 3. We now reference supplementary movie 1 in the results section.